February 6, 1989

Annual Report for Grant No. NAGW-319 Basic
Covering the Period from 15 January 1988 to 14 January 1989

PHOTOABSORPTION AND PHOTODISSOCIATION OF MOLECULES IMPORTANT IN THE INTERSTELLAR MEDIUM

Submitted by:

Long C. Lee and Masako Suto
Department of Electrical & Computer Engineering
San Diego State University
San Diego, California 92182

Prepared for:

NASA Headquarters
Washington, DC 20546

Attention: Dr. Fred C. Gillett
Astrophysics Division
Code EZ

Table of Contents

I. INTRODUCTION

Photoabsorption and fluorescence cross sections of molecules important in the interstellar medium were measured in the 90-200 nm region using synchrotron radiation, excimer laser, and condensed-discharge lamps as light sources. The quantitative spectroscopic data are currently needed for the modeling of formation and destruction rates of molecules by the interstellar radiation field. Fluorescences from excited photofragments produced by vacuum ultraviolet radiation (VUV) of molecules are dispersed to identify the emitting species. The fluorescence data are useful for the identification of emission sources in interstellar clouds.

II. RESEARCH ACCOMPLISHED

The research results accomplished in the period from 15 January 1988 to 14 January 1989 are summarized below:

A. VUV Excitation of HCOOH, $HCOOCH_3$, and CH_3COOH

The photoabsorption and fluorescence cross sections of organic acids (HCOOH, $HCOOCH_3$, CH_3COOH) were measured in the 106-250 nm region using synchrotron radiation as a light source. These molecules have been observed in the interstellar medium. The fluorescence from VUV excitation of these molecules was dispersed to identify the emission source to be from excited OH^* and $HCOO^*$. The results were summarized in a paper (attached as Appendix A) that has been published in the Journal of Physical Chemistry.

B. Fluorescence from VUV Excitation of CH_3

CH_3 is one of the important radicals involving in the interstellar hydrocarbon formation chains. Spectroscopic data relevant to the photodissociation process of this radical are useful for the understanding of hydrocarbon formation process in interstellar clouds. The photoexcitation process of CH_3 was investigated in the reporting period. CH_3 was produced

by the reaction of CH_4 with F or Cl atom in a discharge-flow tube, and then excited by F_2 laser at 157 nm. The CH(A-X, B-X) emissions from photoexcitation of CH_3 were observed. The results are summarized in a paper (attached as Appendix B) that has been published in the Journal of Chemical Physics.

C. Fluorescence from VUV Excitation of $(CH_3)_2O$

$(CH_3)_2O$ is one of the abundant molecules observed in the interstellar medium. The photoabsorption and fluorescence cross sections of this molecule were measured in the 115-195 nm region. Emission was dispersed to identify the emission source to be from the excited photofragment of $CH_3O(\tilde{A})$. The results are summarized in a paper (attached as Appendix C) that has been published in the Journal of Chemical Physics.

D. Photoabsorption and Fluorescence of C_2H_5OH

C_2H_5OH has been observed in the interstellar medium. The photoabsorption and fluorescence cross sections of this molecule were measured in the 46-200 nm region using synchrotron radiation as a light source. The fluorescence observed from VUV excitation of C_2H_5OH was dispersed to identify the emitting species to be from excited OH^*, CH^*, and H^*, depending on excitation wavelength. The results are summarized in a paper (attached as Appendix D) that has been submitted to the Journal of Quantitative Spectroscopy and Radiative Transfer for publication.

E. Fluorescence from VUV Excitation of C_2H_2

C_2H_2 is one of the important hydrocarbon interstellar molecules. The photoabsorption and fluorescence cross sections of C_2H_2 in the 106-200 nm region were reported in previous funding period. The quantitative spectroscopic data in the 50-106 nm region were obtained in this reporting period.Fluorescence observed at various excitation wavelengths was dispersed to identify the emission species to be excited C_2H^*, C_2^*, CH^*, H^*, and possibly

$C_2H_2^{+*}$. The results are summarized in a paper (attached as Appendix E) which has been accepted by the Journal of Chemical Physics for publication.

III. PUBLICATION AND PRESENTATIONS IN THIS REPORTING PERIOD

1. M. Suto, X. Wang, and L. C. Lee, *"Fluorescence Yields from Photodissociative Excitation of HCOOH, $HCOOH_3$, and CH_3COOH in the Vacuum Ultraviolet Region,"* J. Phys. Chem. **92**, 3764 (1988).
2. L. C. Lee and M. Suto, *"Photoabsorption and Fluorescence Cross Sections of Halogen Compounds in VUV,"* Invited paper presented in the section of X-Ray and Vacuum Ultraviolet Interaction--Data bases, calculations, and Measurements, Proceedings of SPIE, Vol 911, p. 39 (1988).
3. C. Ye, M. Suto, and L. C. Lee, *"CH(A, B-X) Fluorescence from VUV Excitation of CH_3,"* J. Chem. Phys. **89**, 2797 (1988).
4. M. Suto, C. Ye, and L. C. Lee, *"$CH_3O(\tilde{A}\text{-}\tilde{X})$ Fluorescence from Photodissociation of Dimethyl Ether,"* J. Chem Phys. **89**, 6555 (1988).
5. J. C. Han, M. Suto, and L. C. Lee, *"Fluorescence from Photoexcitation of C_2H_5OH by Vacuum Ultraviolet Radiation,"* submitted to J. Quant. Spectry. Radiat. Transfer (1989).
6. J. C. Han, C. Ye, M. Suto, and L. C. Lee, *"Fluorescence from Photoexcitation of C_2H_2 at 50-106 nm,"* J. Chem. Phys., in press (1989).

Appendix A

"Fluorescence Yields from Photodissociative Excitation of HCOOH, $HCOOCH_3$, and CH_3COOH in the Vacuum-Ultraviolet Region"

FLUORESCENCE FROM PHOTOEXCITATION OF C_2H_5OH BY VACUUM ULTRAVIOLET RADIATION

J. C. Han, Masako Suto, and L. C. Lee
Molecular Engineering Laboratory
Department of Electrical and Computer Engineering
San Diego State University
San Diego, CA 92182

ABSTRACT

The photoabsorption and fluorescence cross sections of C_2H_5OH are measured in the 46-200 nm region. Fluorescence is dispersed to identify the emission systems, which are mainly OH(A-X), CH(A, B-X), and H Balmer series. The photodissociation processes that produce the observed emissions are discussed.

(8306X)

INTRODUCTION

C_2H_5OH (ethanol) is an interstellar molecule. Its photoabsorption and fluorescence cross sections are of interest for the study of the formation and destruction processes of molecules in interstellar clouds. The spectroscopic data are also needed for understanding the chemical processes occurring in discharge media that contain this molecule. This molecule is potentially useful for plasma-assisted chemical deposition of diamond-like films.

The photoabsorption cross section of C_2H_5OH in the vacuum ultraviolet region has been measured by several investigators in various wavelength regions.[1-4] By contrast, the fluorescence data are scarce. Terenin and Neujmin[5] reported the observation of OH(A-X) from photoexcitation of C_2H_5OH in the 130-150 nm region a while ago. Vinogradov and Vilesov[4] measured the OH(A-X) fluorescence yield (which is quite small) in the 90-130 nm region. The fluorescence cross section and the dispersed fluorescence spectra are reported in this paper.

EXPERIMENTAL

The absorption and fluorescence cross sections were measured using synchrotron radiation as a light source.[6,7] The synchrotron radiation was produced by the 800 MeV electron storage ring at the University of Wisconsin, and it was dispersed by a 1-m Seya-Namioka vacuum monochromator. The high vacuum monochromator was separated from the 40.9 cm long, 3.5 cm I.D. gas cell by a metal film window. A thin Al film was used for the 46-75 nm region, an In film for 74-106 nm, and a LiF crystal for 105-215 nm. The windows also served as optical filters to cut-off the high-order light. The fluorescence was observed by a cooled photomultiplier tube (EMI 9558QB),

sensitive in the 190-800 nm region. The fluorescence and absorption cross sections were measured simultaneously at room temperature (24 ^{o}C).

The fluorescence spectra produced by photoexcitation of C_2H_5OH at a few atomic emissions lines in the 45-130 nm region were dispersed by a 0.3-m monochromator (McPherson 218).[8] The atomic emission lines were produced by a condensed-capillary-discharge light source, and each line was isolated by a 1-m vacuum monochromator (McPherson 225). No windows were placed in the light source path. The fluorescence was detected by a cooled photomultiplier tube (EMI 9558QB), and the signal processed by a gated counting system.

The denatured ethanol liquid (ethyl alcohol) was supplied by the Aldrich Chemical Co. The sample purity was 99.9% and contained 95% 3A alcohol and 5% isopropyl alcohol by volume. The sample was purified by fractional distillation. The vapor pressure of methyl alcohol (CH_3OH) is higher than ethanol at a given temperature; thus, the possible impurity of CH_3OH can be removed by pumping the sample repeatedly through several cycles that range from room temperature to the liquid N_2 temperature. However, isopropyl alcohol has a lower vapor pressure than ethyl alcohol, so its impurities may not be removed. At room temperature the vapor pressure of ethanol is about 60 torr and isopropyl alcohol about 40 torr; thus, the impurity of isopropyl alcohol in the vapor phase could be 3%. Namely, the overall purity of ethanol vapor could be about 97%.

RESULTS AND DISCUSSION

(a) Photoabsorption and fluorescence cross sections

The photoabsorption cross section of C_2H_5OH in the 46-123 and 123-200 nm region is shown in Figs. 1(a), and (b), respectively. The experimental

uncertainty is estimated to be ± 10% of the given value, except for the 70-75 and 98-105 nm regions where the uncertainty could be as high as ± 15% because of distortion by the scattered light. Each absorption cross section was measured at several pressures less than 100 mTorr, depending on the magnitude of the cross section. Our values agree well with the data of Salahub and Sandorfy[3] for wavelengths longer than 120 nm. At the shorter wavelengths, our data are systematically lower than the early measurements,[1,2,4] but the differences are within experimental uncertainties.

The fluorescence cross sections in the 46-62 and 106-112 nm region is shown in Fig. 1(a). The cross section is smaller than 6×10^{-20} cm^2. Since the fluorescence intensity is generally weak, the experimental uncertainty is high (by a factor of 2). The fluorescence cross section was measured with synchrotron radiation. The detection response of the photomultiplier tube (EMI 9556QB) was not corrected. In the 46-62 nm region, the absolute fluorescence cross section was determined by comparing the fluorescence intensity with the $N_2^+(B\text{-}X)$ emission from photoexcitation of N_2, for which the fluorescence cross section is known.[7] In the 106-112 nm region, the emission from photoexcitation of H_2O was used as the calibration standard.[9] In the 74-106 nm region, the synchrotron radiation transmitting through the In film was too weak to measure the fluorescence cross section with a certainty. The fluorescence cross section is estimated to be about the same magnitude as that in the 46-64 nm region.

The fluorescence quantum yield, which is calculated from the ratio of the fluorescence to photoabsorption cross sections, is in the order of 0.1%. The current value is slightly higher than the quantum yield measured by Vinograd and Vilesov[4] that is about 0.04% in the 90-130 nm region. Nevertheless, the difference is within experimental uncertainties.

(b) Fluorescence spectra

The fluorescence spectra from photoexcitation of C_2H_5OH were observed at sixteen excitation wavelengths: 45.7, 52.7, 55.1, 58.7, 63.7, 66.2, 68.5, 76.5, 78.5,83.4, 92.3, 95.5, 99.1, 103.7, 108.4, and 124.9 nm. The sample fluorescence spectra at various wavelengths are shown in Figs. 2-4.

As shown in Fig. 2, the fluorescence observed at excitation wavelengths longer than 100 nm is essentially the OH(A-X) system. Some weak emission bands seem to appear in the 380-520 nm region, but the emitting sources are not identified because of weak intensity. The current result confirms the earlier assertion[4,5] that the emission observed from photoexcitation of C_2H_5OH in the 100-130 nm region is the OH(A-X) band.

In addition to OH(A-X), the CH(A, B-X) emissions appear at 99.1 nm as shown in Fig. 3(a). The CH emission intensity becomes more intense (when compared to OH) at shorter excitation wavelengths, for instance, the spectra for the 92.3 and 76.5 nm excitation are shown in Figs. 3(b) and 3(c), respectively. No emissions other than the OH and CH emissions are detected in the 76-99 nm region.

In addition to the OH and CH emissions, the H(n-2) Balmer series start to appear at 68.5 nm as shown in Fig. 4(a). The shorter the excitation wavelengths, the stronger are the Balmer series; examples are shown in Fig. 4(b) for the 63.7 nm excitation and Fig. 4(c) for 55.1 nm.

The branching ratios for the peak intensities of CH(A-X), H(3-2),and H(4-2) relative to OH(A-X) as a function of excitation wavelengths are plotted in Fig. 5. The combined detection response of the photomultiplier tube and the monochromator was calibrated by a standard halogen lamp and used to correct the peak intensities of the dispersed fluorescence spectra. The ratio of CH(A-X)/OH(A-X) shows a maximum at 78.5 nm, decreases sharply

to a small value at 68.5 nm, and then increases slowly with decreasing excitation wavelength. The emission intensities are the useful information for the study of photodissociation processes as discussed below.

(c) Photodissociation processes

The excitation energies and the wavelength thresholds for the production of fluorescence from photoexcitation of C_2H_5OH are listed in Table I. The threshold excitation energies are calculated from the heats of formation[10-12] and the excitation energies of $OH^*(A)$,[13] $CH^*(A)$,[13] and $H^*(n)$.[14]

$OH^*(A)$ can be produced at a threshold of 154.8 nm by the $C_2H_5+OH^*(A)$ process. However, the OH(A-X) fluorescence appears at wavelengths much shorter than this threshold; the fluorescence yield has a significant value only at wavelengths shorter than 130 nm.[4] The observed OH emission is most likely produced by this dissociative excitation process.

The process responsible for the CH(A, B-X) emissions is not as obvious as that for OH(A-X). Extrapolating the emission intensity ratio of CH/OH to zero, the threshold for the CH(A-X) emission is about 102 nm as shown in Fig. 5. Based on this threshold energy, the possible dissociative excitation processes responsible for the CH(A-X) emission are $CH_3 + CH^*(A) + H_2O$ and $CH^*(A) + H_2 + CH_2OH$, for which the threshold wavelengths are 118.5 and 110.2 nm, respectively.

Extrapolating the emission intensity ratios of H(3-2)/OH(A-X) and H(4-2)/OH(A-X) to zero in Fig. 5, the threshold wavelengths for the production of H^*(n=3 and 4) are about 73 and 70 nm, respectively. These threshold wavelengths suggest that the H Balmer series are most likely produced by the $C_2H_5O + H^*(n)$ processes, for which the threshold wavelengths for the production of H^*(n=3 and 4) are calculated to be 74.6 and 71.8 nm,

respectively. The possibility that the excited H^* atoms are produced by the $C_2H_4OH + H^*(n)$ is not ruled out.

The ionization yield in the 90-118 nm region is much smaller than 1.[2,15] Thus, the quantum yield for dissociation into neutral products must be quite large, for instance, the quantum yield for neutral products is 75% at 106 nm.[2] Since the measured quantum yield for the UV and visible fluorescence is very small (less than 0.1%), the excited $C_2H_5OH^*$ must decay into vibrationally-excited products that may subsequently emit infrared radiation. It is of interest to observe the IR emission that may provide vital information for a further study of the photodissociation process.

The fluorescence spectra (Figs. 2-4) show emissions only from the excited OH^*, CH^*, and H^* species, implying that emissions from excited $C_2H_5OH^{+*}$ ion state are extremely small. Several excited ion states were observed[16] in the 58.4 nm photoelectron spectrum of C_2H_5OH. However, the bandwidths of the excited ion states are so broad[16] that the excited states are most likely predissociated, namely, emissions from the excited ions are expected to be small.

CONCLUDING REMARKS

The photoabsorption and fluorescence cross sections of C_2H_5OH were measured in the 46-200 nm region. At excitation wavelengths longer than 100 nm, the observed emission is solely the OH(A-X) system. The CH(A, B-X) emissions are observed at excitation wavelengths shorter than 100 nm. The H^* Balmer series are observed at excitation wavelengths shorter than 68.5 nm. The emission from excited $C_2H_5OH^{+*}$ states are negligible. The observed UV and visible fluorescence quantum yields are in the order of 0.1% which is much smaller than the quantum yield for the neutral products. The VUV

excitation of C_2H_5OH may emit infrared radiation that is of interest for further study.

ACKNOWLEDGEMENT

This work is based on research supported by the NASA and the NSF. The synchrotron radiation facility at the University of Wisconsin is supported by the NSF.

REFERENCES

1. M. Ogawa and G. R. Cook, J. Chem. Phys. **28**, 747 (1958).
2. J. C. Person and P. P. Nicole, J. Chem. Phys. **55**, 3390 (1971); ibid, Argonne National Laboratory Report, ANL-75-3 part I (1974).
3. D. R. Salahub and C. Sandorfy, Chem. Phys. Lett. **8**, 71 (1971).
4. I. P. Vinogradov and F. I. Vilesov, Khimiya Vysokikh Énergii, **11**, 25 (1977).
5. A. Terenin and H. Neujmin, J. Chem. Phys. **34**, 436 (1935).
6. L. C. Lee, R. W. Carlson, and D. L. Judge, J. Phys. B: At. Mol. Phys. **9**, 855 (1976).
7. L. C. Lee, J. Phys. B: At. Mol. Phys. **10**, 3033 (1977).
8. L. C. Lee, X. Wang, and M. Suto, J. Chem. Phys. **85**, 6294 (1986).
9. L. C. Lee and M. Suto, Chem. Phys. **110**, 161 (1986); L. C. Lee, J. Chem. Phys. **72**, 4334 (1980).
10. S. W. Benson, *Thermochemical Kinetics*, John Wiley, New York (1976).
11. M. W. Chase, Jr., C. A. Davies, J. R. Downey, Jr., D. J. Frurip, R. A. McDonald, and A. N. Syverud, J. Phys. Chem. Ref. Data, Vol. 14, Suppl. No. 1 (1985).
12. J. M. Dyke, A. R. Ellis, N. Jonathan, N. Keddar, and A. Morris, Chem. Phys. Lett. **111**, 207 (1984).
13. K. P. Huber and G. Herzberg, *Constants of Diatomic Molecules*, (Van Nostrand, New York 1979).
14. C. E. Moore, *Atomic Energy Levels*, NSRDS-NBS 35, Natl. Bur. Stand. Washington, DC 20025 (1971).
15. K. M. A. Refaey and W. A Chupka, J. Chem. Phys. **48**, 5205 (1968).
16. M. B. Robin and N. A. Kuebler, J. Electr. Spectrosc. Rel. Phenom. **1**, 13 (1972/73).

Table I Threshold excitation energies and threshold wavelengths for photodissociation of C_2H_5OH into excited photofragments

Process	Energy (eV)	Wavelength (nm)
$C_2H_5 + OH^*(A)$	8.01	154.8
$CH_3 + CH^*(A) + H_2O$	10.46	118.5
$CH^*(A) + H_2 + CH_2OH$	11.25	110.2
$C_2H_5O + H^*(n=3)$	16.61	74.6
$C_2H_5O + H^*(n=4)$	17.27	71.8

FIGURE CAPTIONS

Fig. 1. Photoabsorption (solid line) and fluorescence (dash line) cross sections of C_2H_5OH in units of Mb (10^{-18} cm^2). The spectral resolution is 0.2 nm.

Fig. 2. Fluorescence spectra of C_2H_5OH excited at (a) 124 nm, (b) 108.4 nm, and (c) 103.7 nm. The spectral resolution was 4 nm. The gas pressures were 15 mTorr for (a) and 20 mTorr for (b) and (c).

Fig. 3. Fluorescence spectra of C_2H_5OH excited at (a) 99.1 nm, (b) 92.3 nm, and (c) 76.5 nm. The spectral resolution was 2.5 nm. The gas pressures were 15 mTorr for (a) and 20 mTorr for (b) and (c).

Fig. 4. Fluorescence spectra of C_2H_5OH excited at (a) 68.5 nm, (b) 63.7 nm and (c) 55.1 nm. The spectral resolutions were 3 nm for (a) and (b) and 1.5 nm for (c). The gas pressure was 20 mTorr.

Fig. 5. Branching ratios of the peak emission intensities of the CH(A-X), H(3-2), and H(4-2) emission bands relative to OH(A-X) by excitation of C_2H_5OH at various excitation wavelengths. The intensities are corrected with the detection response.

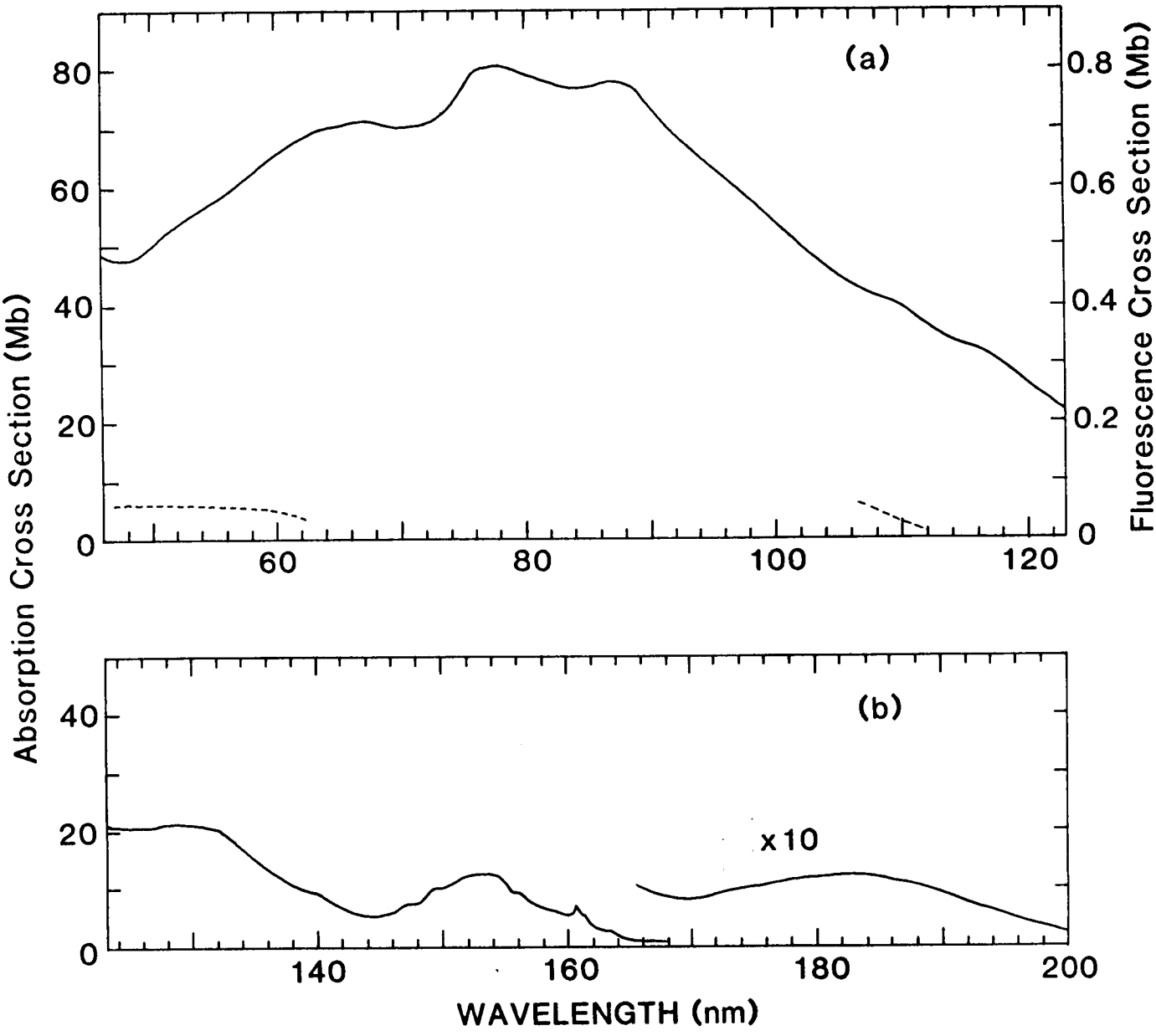
(a)
(b)
x10
Absorption Cross Section (Mb)
Fluorescence Cross Section (Mb)
WAVELENGTH (nm)
0
20
40
60
80
0.2
0.4
0.6
0.8
100
120
140
160
180
200

Fig. 1

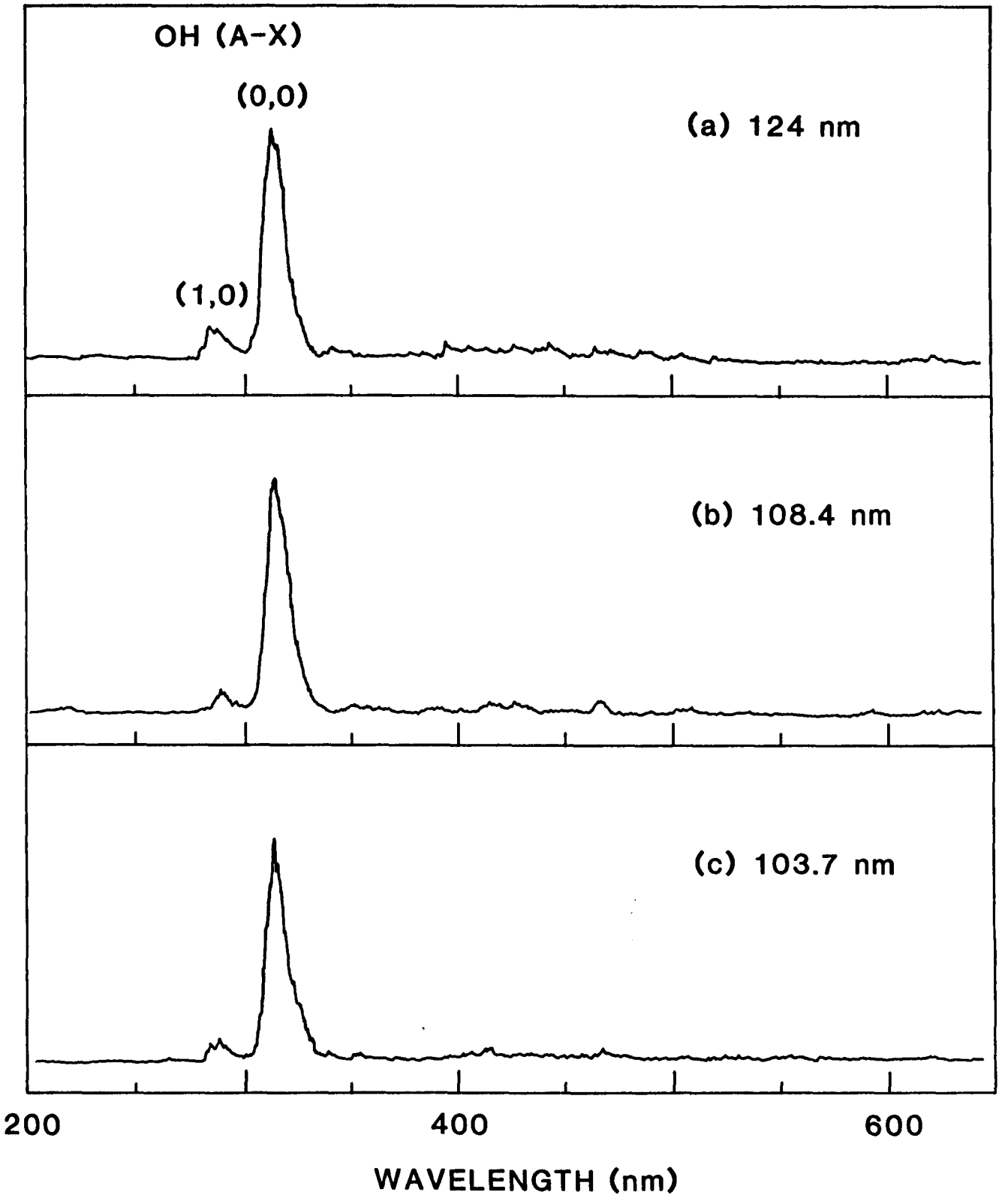

Fig. 2

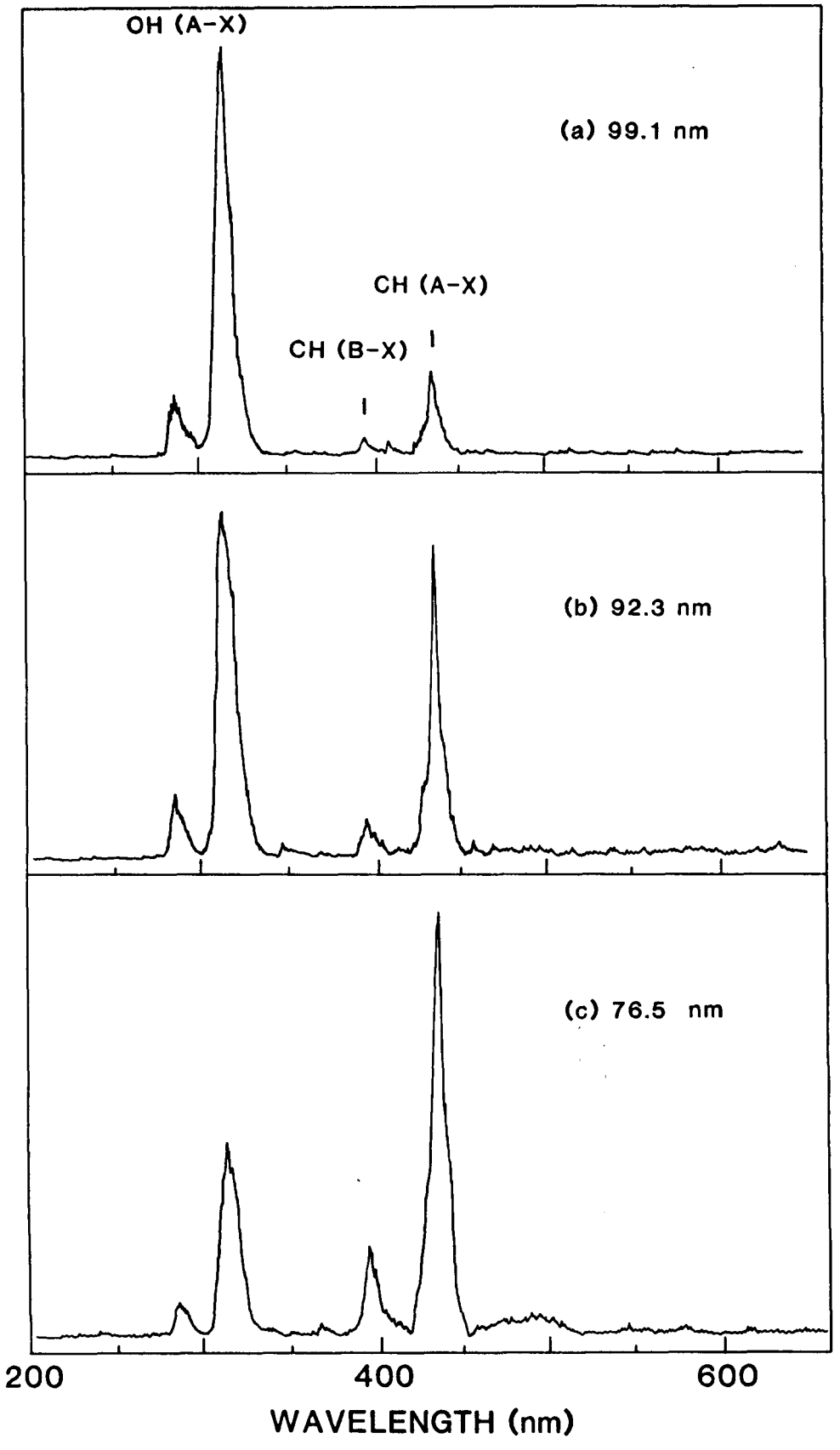
OH (A-X)
(a) 99.1 nm
CH (A-X)
CH (B-X)
(b) 92.3 nm
(c) 76.5 nm
200
400
600
WAVELENGTH (nm)

Fig. 3

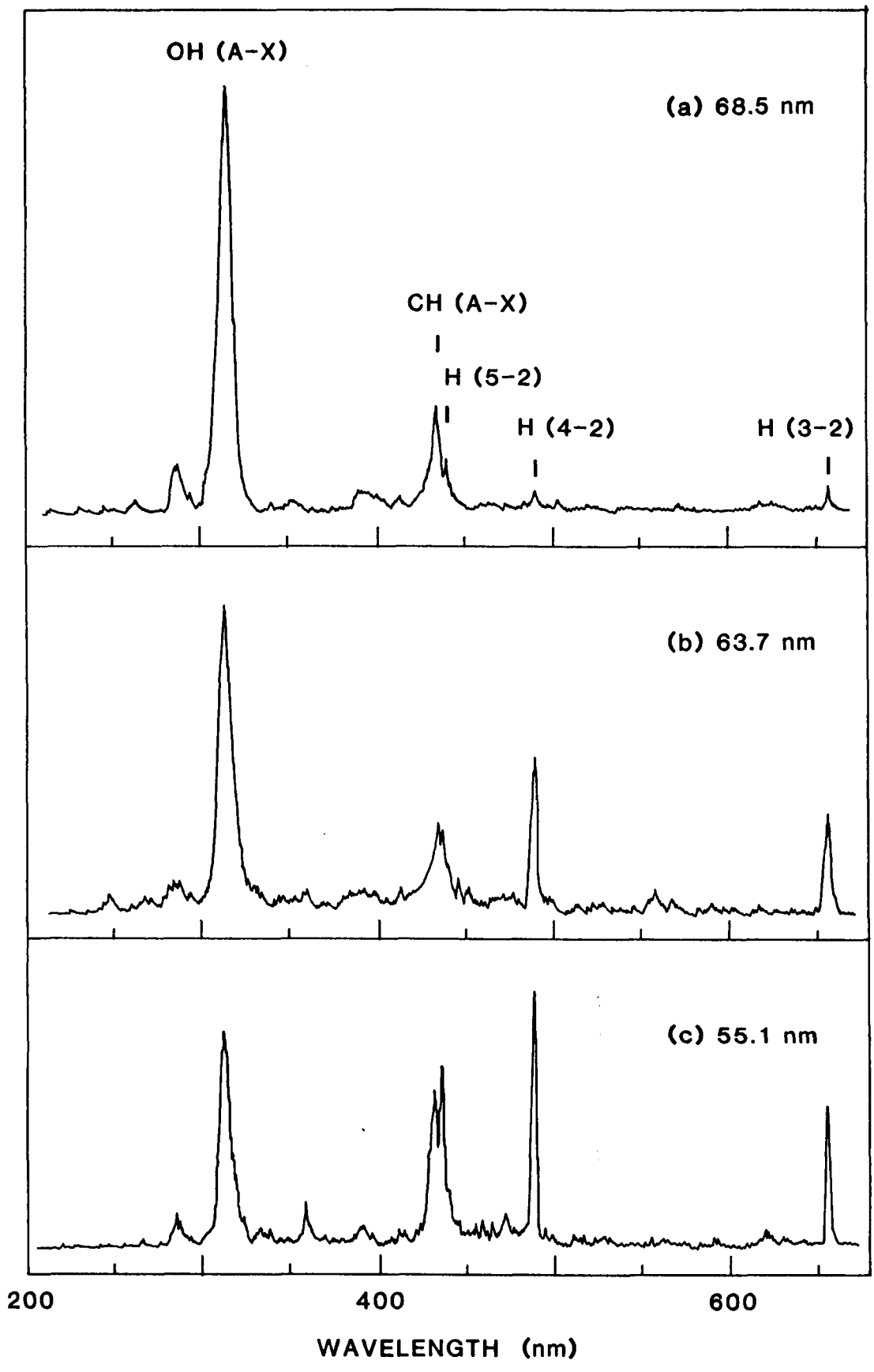
OH (A-X)
(a) 68.5 nm
CH (A-X)
H (5-2)
H (4-2)
H (3-2)
(b) 63.7 nm
(c) 55.1 nm
200
400
600
WAVELENGTH (nm)

Fig. 4

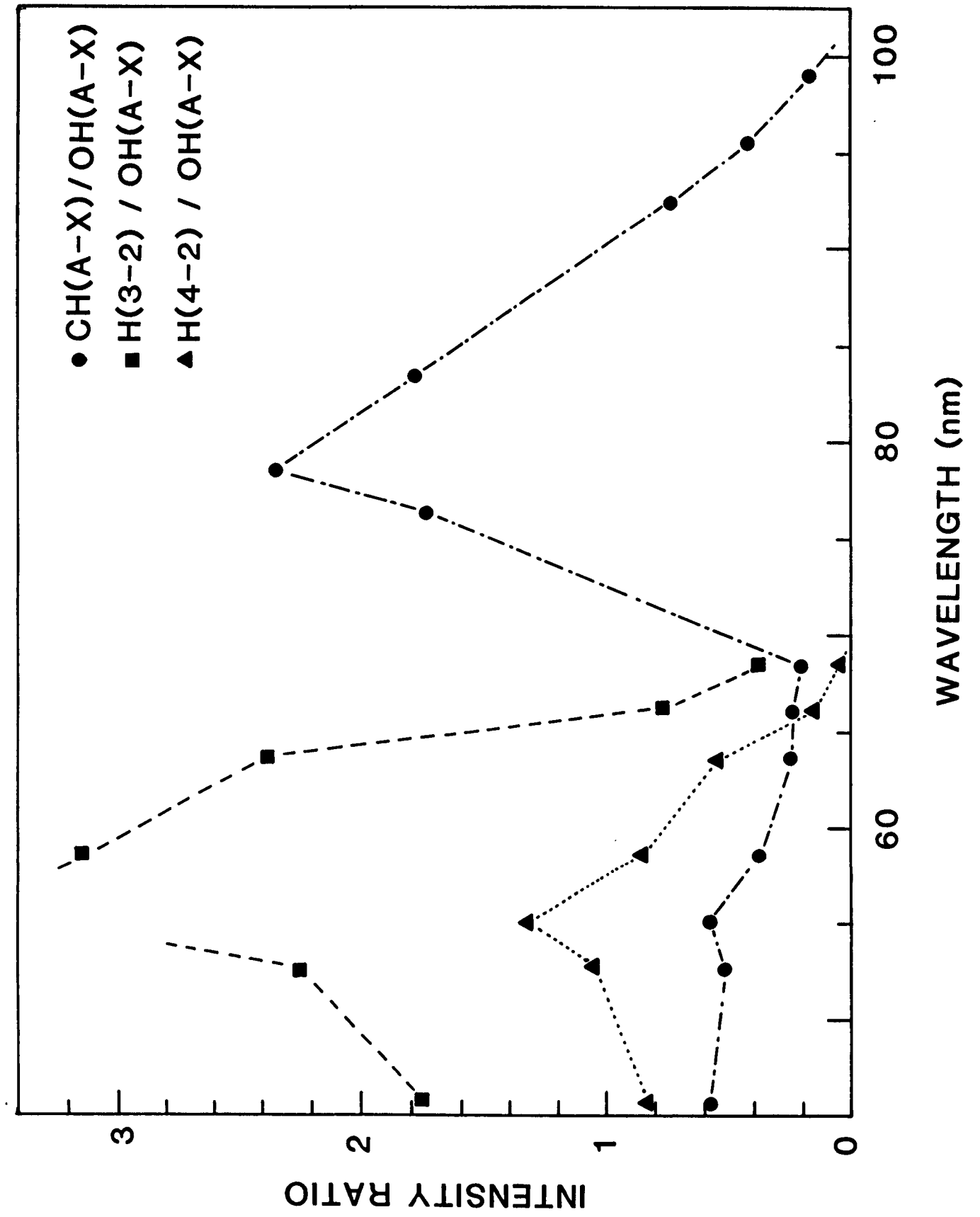
● CH(A–X) / OH(A–X)
■ H(3–2) / OH(A–X)
▲ H(4–2) / OH(A–X)
INTENSITY RATIO
0
1
2
3
60
80
100
WAVELENGTH (nm)

Fig. 5

Appendix E

"Fluorescence from Photodissociation of C_2H_2 at 50-106 nm."

Fluorescence from Photoexcitation of C_2H_2 at 50-106 nm

J. C. Han, Chao Ye, Masako Suto, and L. C. Lee
Molecular Engineering Laboratory
Department of Electrical and Computer Engineering
San Diego State University
San Diego, CA 92182

ABSTRACT

The photoabsorption and fluorescence cross sections of C_2H_2 were measured in the 50-106 nm region using synchrotron radiation as a light source. Fluorescence observed at several excitation wavelengths was dispersed to identify the fluorescing species that are excited C_2H^*, C_2^*, CH^*, H^*, and possibly $C_2H_2^{+*}$. The photodissociation process of C_2H_2 leading to the formation of fluorescing species is discussed. The C_2(C-A) emission observed at 92.3 and 95.5 nm is produced by the molecular elimination process associated with superexcited state(s). Fluorescence spectra from the two-photon excitation of C_2H_2 at 157.5 and 193 nm were also observed and compared with those of single-photon excitation at the equivalent excitation energies.

(8237.X)

I. INTRODUCTION

C_2H_2 and its photodissociation fragments are important in the studies of interstellar photochemistry, combustion chemistry, and atmospheric chemistry. Currently, C_2H_2 is also used for chemical vapor deposition of diamond film. These applications stimulate interest for the study of its photodissociation processes.

The photochemistry of C_2H_2 has been extensively studied in the 106-200 nm region.[1-3] Emission from the excited CH_2^* radical was observed from dissociative excitation of C_2H_2 at wavelengths shorter than 136.5 nm,[2,3] and the fluorescence cross section for the visible emission was measured.[3] In the 50-106 nm region, the photodissociation processes are not well studied, in contrast to the extensive study of photoionization processes.[4-11] The ionization yield in the 70-100 nm region is much less than 1 (between 0.6 and 0.8),[4] indicating that a substantial fraction of the superexcited $C_2H_2^{**}$ decays to neutral products. (The neutral excited state at an energy higher than the first ionization threshold is called a superexcited state). The superexcited states in this wavelength region have been extensively studied both experimentally[7-11] and theoretically.[7,8,11-13] The superexcited states may lead to excited photofragments that subsequently emit. Thus, fluorescence is an important character of superexcited state(s) that is the subject of the current study. Fluorescence was dispersed to identify spectra of emitting species and used to study the photodissociation processes. In addition, the fluorescence spectra produced by the two-photon excitation of C_2H_2 at 193 and 157.5 nm were observed and compared with those of single-photon excitation at equivalent energies.

The quantitative absorption and fluorescence cross sections are the most basic data for studying molecular photodissociation processes. The

absorption cross section of C_2H_2 was measured by Metzger and Cook[4] in the 60-100 nm region and by Wu and Judge[14] in the 17.5-74 nm region. Emission from photoexcitation of C_2H_2 was reported and relative fluorescence quantum yield was measured.[4] The photofragment emission produced at 73.59 nm was dispersed, and the emission system identified to be the CH(A, B-X) and C_2 Swan bands.[15] The fluorescence quantum yield at this excitation wavelength was estimated[15] to be 0.1%. This fluorescence yield is too small to account for the neutral product yield which is about 10% at this wavelength.[4] In contrast, the currently measured fluorescence yield is about 5%; thus, the neutral excited state has a substantial fraction decayed through fluorescence. The absolute photoabsorption and fluorescence cross sections as well as the fluorescence quantum yield in the 50-106 nm region are reported in this paper.

II. EXPERIMENTAL

The experimental apparatus and procedure were described in previous publications.[16,17] In short, synchrotron radiation provided by the electron storage ring at the University of Wisconsin was used as a light source for absorption and fluorescence cross section measurements. Radiation was dispersed by a 1-m Seya monochromator. Three different windows[18] (LiF crystal for $\lambda > 105$ nm, In thin film for 74-106 nm, and Al thin film for 50-75 nm) were used to separate a gas cell from the high vacuum monochromator. The windows also served as optical filters to cut off the higher orders of light that could interfere with the measurements. The gas cell was a stainless steel tube of 3.5 cm I.D. and 40.9 cm long. Sample gas was slowly pumped by a sorption pump. Fluorescence was observed by a photomultiplier tube (EMI 9558QB).

A capillary-condensed-discharge light source was used for the experiment of fluorescence dispersion.[16] Each atomic emission line was isolated by the 1-m vacuum monochromator before entering the (3" I.D., 5" long) gas cell. No windows were used in the light source path. Fluorescence was dispersed by a 0.3-m monochromator.

An excimer laser (Lumonics TE860-4) was used for the two-photon excitation measurements.[17] The gas cell was a (4" O.D. six-way) stainless steel cross with a MgF_2 window placed in front of the excimer laser beam. For the transmission of F_2 laser light (157.5 nm), high purity nitrogen was used to continuously flush the MgF_2 windows between the F_2 laser and the gas cell. The power for the ArF (193 nm) laser was monitored by a power meter. The relative power of the F_2 laser was monitored by measuring the fluorescence intensity from the excited photofragments of C_2F_3Cl.[19] Fluorescence was dispersed by a 0.25-m spectrometer and detected by a gated 1024 channel diode array (OMA III, EG&G PARC).

C_2H_2 was supplied by Matheson with a purity of at least 99.6%. The gas was used as delivered.

III. RESULTS AND DISCUSSION

A. *Absorption and Fluorescence Cross Sections*

The photoabsorption cross section of C_2H_2 in the 50-106 nm region measured with a resolution of 0.2 nm is shown in Fig. 1(a). The cross section was measured by the attenuation of light source intensity by C_2H_2 at several pressures lower than 30 mTorr, where the absorbance of $\ln(I_o/I)$ depends linearly on the gas pressure. The experimental uncertainty is estimated to be within 10% of the given value. At the edges of the windows (73-75 and 104-106 nm), the uncertainties could be as high as 15%. The

present data agree well with the measurement of Metzger and Cook[4] in the 70-100 nm region. In the 58-70 nm region, the present data are higher than the values of Metzer and Cook[4], but they agree well with those of Wu and Judge.[14] In the 100-106 nm region, there are no published data available for comparison with the present measurement, except for the datum at 106 nm (24.5 Mb) that agrees with the previous value.[3]

Wu and Judge[14] observed two Rydberg series in the 65-70 nm region converging to the $B^2\Sigma_u^+$ state of $C_2H_2^+$. Such structures are shown in the present spectrum in spite of low resolution. In the 70-98 nm region, a number of sharp structures superimpose on two broad bands peaked at 80 and 92 nm as shown in Fig. 1(a). These characteristic features were previously observed in both photoabsorption and ionization spectra,[5,6,11] and they were assigned to Rydberg states.[11,12] The wavelength positions for the transitions of $3\sigma_g \rightarrow np\sigma_u$ and $np\pi_u$, $2\sigma_u \rightarrow ns\sigma_g$ and $nd\pi_g$, and $2\sigma_g \rightarrow np\sigma_u$ and $np\pi_u$ calculated by Langhoff *et al.*[12,13] are indicated in Fig. 1(a) for comparison. The intravalance transitions, $2\sigma_u \rightarrow 1\pi_g(\pi^*)$ and $4\sigma_g$ (n/σ^*), are calculated to be in the 13-18 eV region.[12,13]

Fluorescence from photoexcitation of C_2H_2 was observed in the entire wavelength region studied. The fluorescence intensity was converted to absolute cross section by comparing it with the fluorescence of N_2 and CO for which the fluorescence cross sections are known.[20,21] The $N_2^+(B\text{-}X)$ emission occurs at excitation wavelengths shorter than 66.1 nm,[20] which was used to calibrate the fluorescence in the Al film region. The $CO^+(A\text{-}X)$ emission occurs at wavelengths shorter than 75 nm,[21] which was used to calibrate the fluorescence observed in the In film region. The fluorescence cross section was measured at low pressures (typically < 1 mTorr) so that the fluorescence intensity was linearly dependent on the pressure. The

fluorescence cross section is shown in Fig. 1(a). The experimental uncertainty is estimated to be ± 30% of a given value.

The quantum yield for the production of fluorescence is calculated as the ratio of the fluorescence cross section to the absorption cross section as shown in Fig. 1(b). The quantum yield shows three distinct peaks at 68, 75, and 85 nm. This profile is very similar to the relative fluorescence yield measured by Metzger and Cook.[4] The quantum yield has a maximum of 5% at 75 nm. The quantum yield is much higher than the previous value of about 0.1% measured at 73.59 nm.[15]

It was noted[4] that the wavelengths for the maxima in the fluorescence yield curve correlates fairly well with those of the minima in the ionization yield curve. This assertion is confirmed in the current results, which vividly show that the minima of the fluorescence yield at 80 and 96.5 nm correspond to the maxima of photoionization yield measured by Hayaishi, *et al.*[11] and vice versa at 86 nm. These results indicate that the fluorescence process is complementary with the autoionization process; that is, a molecule is first excited to a superexcited state that subsequently decays to an excited photofragment or autoionizes to a $C_2H_2^+$ ion.

The superexcited states that consist of the Rydberg and/or valence states exist in the 78-91 nm region.[11-13] The oscillator strengths for the sum of the $3\sigma_g \rightarrow np\sigma_u$ and $np\pi_u$ Rydberg transitions in this wavelength region was calculated to be $f \geq 0.227$ by Hayaishi *et al.*[11] and $f = 0.306$ by Langhoff *et al.*[12] These values are one order of magnitude larger than the current fluorescence oscillator strength that is $f = 0.030$ in the 78-95 nm region.

The dependence of fluorescence intensity on gas pressure was observed to examine the quenching effect of the excited states. As an example, the results at excitation wavelengths of 60, 70, 80, and 100 nm are shown in

Fig. 2. The fluorescence intensities are linearly dependent on gas pressures below 10 mTorr at excitation wavelengths longer than 74 nm, but they are severely quenched at shorter wavelengths. The quenching was observed even at gas pressures less than 0.5 mTorr. Due to such a large quenching effect, the fluorescence cross sections at shorter wavelengths have a large uncertainty. The quenching data clearly indicates that the emitting species produced at shorter excitation wavelengths are different from those at longer wavelengths. It is of interest to identify the emitting species by dispersing fluorescence.

B. Fluorescence Spectra

Fluorescence spectra produced at thirteen excitation wavelengths were given as shown in Figs. 3-8. Possible photodissociation processes relevant to the fluorescence are listed in Table. I. The threshold energies are calculated from the dissociation energies based on the heats of formation[22] and the electronic energies[23,24] of excited fragments. The observed excitation wavelengths that start to produce emissions from specific excited photofragments are also listed in Table I. The electronically-excited photofragments observed at various excitation wavelengths are listed in Table II.

A visible continuum band was observed at excitation wavelengths of 124 and 99.1 nm as shown in Fig. 3(a) and (b), respectively. Both spectra are essentially the same except that the maximum intensity is shifted to the blue as the excitation energy increases. This emission is identified as the $C_2H(\tilde{B}\text{-}\tilde{X})$ transition previously observed[2,25-27] from the photolysis of C_2H_2 at excitation wavelengths longer than 106 nm. The fluorescence spectrum extends to the IR region,[27] but in the present experiment the fluorescence is limited to the visible region because of low response of the photo-

multiplier tube in the IR region. The excited species is essentially produced through the dissociative state that correlates with the C_2H^*+H products as discussed in the previous paper.[3] The threshold of this dissociation process is observed at 136.5 nm,[3,27] and the maximum quantum yield for the visible fluorescence is 13% at 112 nm.[3] The quantum yield decreases with decreasing excitation wavelength [see Fig. 1(b)], because the excitation energy moves away from the Franck-Condon region of the dissociative state.

The fluorescence cross section increases when excitation wavelengths are shorter than 97 nm. Fig. 4(a) shows the spectrum excited at 95.5 nm, where a sharp peak identified as the CH(A-X) transition appears at 432 nm, in addition to the C_2H^* emission. According to the energy thresholds listed in Table I, the CH(A-X) emission observed at 95.5 nm is due to the dissociation process, $C_2H_2 + h\nu \rightarrow CH^*(A^2\Delta) + CH(X^2\Pi_r)$. A weak emission band identified to be the $C_2(C^1\Pi_g \rightarrow A^1\Pi_u)$ transition is also observed at 95.5 nm, which is due to the dissociation process, $C_2^*(C) + H_2$, in accord with the dissociation energy threshold. The photon energy is not sufficiently large enough to produce $C_2^*(C)$ + 2H, which has a threshold at 82 nm.

In addition to the CH(A-X) and C_2(C-A) bands, the $C_2(d^3\Pi_g \rightarrow a^3\Pi_u)$ emission is also observed at 92.3 nm as shown in Fig. 4(b). The $C_2^*(d)$ excited state is presumably produced by the C_2^* + 2H process. The photon energy (13.43 eV) is only slightly higher than the energy threshold of the dissociation process (13.34 eV); thus, the $C_2^*(d)$ is mostly excited in the v = 0 level. This explains why the C_2(d-a) (0,0) transition is the strongest one. The photon energy is sufficiently large to produce the excited $CH^*(B^2\Sigma^-)$ species by the $CH^*(B)$ + CH(X) process, and the CH(B-X) emission band is observed as shown in Fig. 4(b). A single band with a peak

at 231 nm was also observed at this and shorter excitation wavelengths. This emission band is presumably the C_2(D-X) emission at 231.3 nm.[23] The C_2^*(D) is produced by the C_2^*(D) + H_2 process. The relative emission intensities for the C_2(C-A) to the CH(A-X) bands are about the same at 95.5 and 92.3 nm, but the C_2H^* emission becomes weaker at shorter wavelengths. The C_2H^* emission intensity decreases systematically with decreasing excitation wavelength.

The fluorescence spectrum produced at 83.4 nm is shown in Fig. 5(a). The CH(C-X) band shows up in addition to the CH(A, B-X) bands. The C_2(d-a) band remains, but the intensity of the $\Delta v = 1$ sequence (that is a combination of the $v + 1 \rightarrow v$ transitions) becomes stronger than that of the $\Delta v=0$ sequence, in difference from the 92.3 nm excitation. The C_2H^* emission disappears, and the C_2(C-A) emission becomes very weak in comparison to the CH(A-X) band.

The C_2(C-A) emission shows up again at 76.5 nm as shown in Fig. 5(b). This emission is likely produced by the C_2^*(C) + 2H process. The C_2(d-a) emission increases and is comparable to the CH(A-X) band. This increase of the C_2(d-a) emission is correlated with the peak of the fluorescence cross section at 76 nm [see Fig. 1(b)]. For the purpose of spectral identification, the spectrum is given with a higher resolution (0.25 nm instead of 1.25 nm) as shown in Fig. 6. The wavelength positions of the Deslandres-d'Azambuja system, C_2(C-A), Swan system, C_2(d-a), and CH(A, B-X) bands are compared with the observed spectrum as indicated in Fig. 6. The observed emission bands are well identified. The C_2 and CH emission bands were also observed at 73.59 nm.[15]

The fluorescence spectrum observed at 68.5 nm is shown in Fig. 5(c). The CH emission remains at the same intensity, but both the C_2(C-A) and

C_2(d-a) emission intensities have decreased greatly. The fluorescence spectra observed at 66.2 and 63.7 nm are very similar to this spectrum, except for the intensities of the C_2 bands which have decreased even more.

The fluorescence quantum yield shown in Fig. 1(b) has a minimum around 62 nm, and then increases at shorter wavelengths. This increase indicates the open-up of a new fluorescence channel. The fluorescence spectra produced at 58.7, 55.1, and 52.7 nm are shown in Figs. 7(a-c), respectively. The hydrogen Balmer series appear, and the C_2(C-A) and C_2(d-a) bands become weak. According to the energy thresholds listed in Table I, the energy threshold for the H_α (n=3→2) line is at 73.1 nm for the $C_2H + H^*$ (n=3) process. However, the Balmer series are not observed even at 63.7 nm. The Balmer series observed at 58.7 nm are up to n=6. The Balmer series become more intense at 55.1 and 52.7 nm. An emission continuum in the 450-650 nm region starts to show up in this wavelength region. This emission continuum becomes more intense at shorter excitation wavelengths as discussed below.

The fluorescence spectrum at 45.7 nm is shown in Fig. 8. The CH(A-X) band and the hydrogen Balmer series remain, and the emission continuum in the 450-650 region becomes prominent. The excited species that emit this continuum emission are not clear. The pressure dependence of total fluorescence intensity shows that the fluorescence at wavelengths shorter than 70 nm is subject to quenching even at pressures as low as 0.5 mTorr (see Fig. 2). The C_2^* and CH^* emission bands are not quenched as evident by the fact that the fluorescence intensity at wavelengths longer than 80 nm is linearly dependent on pressure (see Fig. 2). The lifetimes of the $H^*(n\geq3)$ are very short and they are not expected to be quenched. Therefore, the high quenching rate is likely associated with the emission continuum. To explain such a high quenching rate, the emitting species could be excited

ions or neutral molecules in metastable states. Considering the high excitation energy, the emission is most likely due to excited ions. The $C_2H_2^+$ ($\tilde{A}^2\Sigma_g$ - $\tilde{X}^2\Pi_u$) and $C_2H_2^+$ ($\tilde{B}^2\Sigma_u$ - $\tilde{A}^2\Sigma_g$) transitions[28] are optically-allowed. The $C_2H_2^{+*}(\tilde{A}, \tilde{B})$ excited states show vibrational structures in the photoelectron spectrum of 58.4 nm.[29] Thus, these excited ion states are stable and may fluoresce. However, the Franck-Condon factor for the production of these excited ions is very small,[29] so their fluorescence cross sections are expected to be small.

C. Photodissociative Excitation Processes

According to the fluorescence cross section, quantum yield, and emission spectra, the photodissociative excitation processes of C_2H_2 can be generally divided into three spectral regions: (i) $\lambda > 97$ nm, (ii) $62 \leq \lambda \leq 97$ nm, and (iii) $\lambda < 62$ nm. For excitation wavelengths longer than the threshold (96.6 nm) of the $CH^*(A) + CH(X)$ process, the fluorescence is solely due to C_2H^* that is produced through a dissociative state discussed in a previous paper.[3] The C_2H^* emission is continuously observed at shorter excitation wavelengths, and it disappears at 83.4 nm (see Fig. 5(a)). The C_2^* emissions are not produced in the $\lambda > 99$ nm region, although the dissociation processes of C_2^* (d, C, D)+H_2 are energetically allowed.

The CH(A-X) emission appears right at the threshold of the $CH^*(A) + CH(X)$ process. The increases of the fluorescence cross section and quantum yield at $\lambda < 97$ nm (see Fig. 1) are likely due to this dissociative excitation process. It is surprising that the CH(A-X) emission is very strong, although this dissociation process requires a break of triple bond.

The C_2(C-A) emission observed at 95.5 nm is produced by the molecular elimination process, $C_2^*(C) + H_2$. The threshold for the molecular elimination process is calculated to be 117.2 nm, but the C_2(C-A) emission

does not appear even at 99.1 nm. The appearance of C_2(C-A) at 95.5 nm is likely related to the superexcited state(s). The $C_2H_2^*$ that leads to C_2^* + H_2 must be cis-bent. This bent geometry is quite different from those of C_2H_2 in the ground state and most Rydberg states that are linear. This bent state is likely associated with the superexcited state(s) located in the 85-96 nm region.[7-13] A superexcited state is attributed to the $2\sigma_u \rightarrow 1\pi_g(\pi^*)$ intravalence transition.[12,13] Excitation of an electron to the $1\pi_g(\pi^*)$ orbital could excite C_2H_2 to a cis-bent state.[30-33] The autoionization of the superexcited state(s) into a bent mode of $C_2H_2^+$ ion was observed in the photoelectron spectra by Parr *et al*.[9] The superexcited states may also predissociate into the emitting C_2^*(C). This assertion is supported by the fact that the fluorescence yield and the autoionization yield are complementary.

The C_2^*(d) is not produced at 95.5 nm by the molecular elimination process. This negative result may be due to the fact that the dissociation of C_2H_2 into $C_2^*(d^3\Pi_g)$ + $H_2(X^1\Sigma_g^+)$ is a spin-forbidden process. The C_2(d-a) emission observed at 92.3 nm and shorter wavelengths must be produced by the C_2^*(d) + 2H(^{2}S) process which is spin-allowed. The C_2(d-a) and C_2(C-A) emissions observed at 76.5 nm are so intense that they are likely associated with the superexcited states related to the $2\sigma_u \rightarrow 4\sigma_g(n/\sigma^*)$ intravalence transition.

The fluorescence quantum yield starts to increase at 62 nm (see Fig. 1), which is contributed by the hydrogen Balmer series as shown in Fig. 7. The observed threshold wavelength is much shorter than the calculated one. This large energy difference indicates that the photodissociation fragments carry large excess energies (translational, vibrational, rotational and/or electronic energy). Further analysis of the energy carried by the

photofragments is of interest. The dissociation energy of $D(HC_2-H)$ measured by Wodtke and Lee[34] is 132 ± 2 kcal/mol, which is higher than the value[22] of 112 kcal/mol used in the threshold calculation. This higher dissociation energy will make the observed threshold closer to the calculated threshold [e.g. 69.6 nm for H(n=3)].

D. Multiphoton Excitation of C_2H_2

Fluorescence from multiphoton excitation of C_2H_2 was also observed for comparison with that of single-photon excitation. Since the selection rules for multiphoton excitation are different from those of single-photon excitation, it is expected that their fluorescence spectra at equivalent excitation energies are different.

Mixtures of 15 mTorr C_2H_2 in 1-6 Torr He were irradiated by the unfocused ArF laser beam (193 nm). The emission spectrum is shown in Fig. 9(a). The CH(A-X) and CH(B-X) bands were observed. Weak emission bands appear in the 450-700 nm region that may include some C_2^* emission, but the identification is not certain. The CH(A-X) fluorescence intensity depends quadratically on the laser power, indicating a two-photon excitation process. The energy of two 193 photons is equivalent to a single photon of 96.5 nm that is near the wavelength of 95.5 nm [Fig. 4(a)]. The CH(A-X) band that is produced by a direct dissociation process is prominent in both fluorescence spectra of the one- and two-photon excitations. The C_2(C-A) emission is observed in the single-photon excitation, but not in the two-photon excitation; that is, the two-photon excitation does not promote the molecular elimination process. The C_2H^* emission observed from the single-photon excitation at 95.5 nm is also not shown in the spectrum of the two-photon excitation at 193 nm. As expected, the fluorescence spectra by one- and two-photon excitations are produced through different excited

states in spite of equivalent excitation energies.

The fluorescence spectrum from multiphoton excitation of C_2H_2 has been observed by McDonald, *et al.*[35] using a focused ArF excimer laser beam. They have observed the C_2(A-X) and the CH(A-X) bands from the two-photon excitation of C_2H_2, and observed the C_2(d-a) and C_2(C-A) bands from three-photon excitation. Later, Okabe *et al.*[36] confirmed their results. In the current experiment, the emission due to three photon processes was extremely weak, because the laser was not focused. Also, the C_2(A-X) band was not detected because the detection system (OMA) is not sensitive in the IR region.

The fluorescence spectrum produced by irradiation of the mixtures of 20 mTorr C_2H_2 in 1 Torr He by the unfocused F_2 laser beam (157.5 nm) is shown in Fig. 9(b). The fluorescence was produced by a two-photon excitation process with an equivalent single-photon wavelength at 78.8 nm. Both the C_2 Swan band and the CH(A-X) band were observed; the intensity of the former is stronger than the latter. This fluorescence spectrum is quite different from those produced by one-photon wavelengths at 76.5 and 83.4 nm as shown in Figs. 5(a) and 5(b). In the one-photon excitation, the CH(A-X) band is more intense than the C_2 Swan system. The C_2(C-A) emission observed at 76.5 nm is not observed in the fluorescence spectrum by two-photon excitation at 157 nm, indicating that two-photon excitation does not reach the super-excited state(s). Again, the fluorescence spectra by one- and two-photon excitations are produced through different excited states.

IV. Concluding Remarks

The photoabsorption and fluorescence cross sections of C_2H_2 are measured in the 50-106 nm region. The fluorescence spectra produced at various excitation wavelengths are dispersed to identify the emission systems. For excitation wavelengths longer than 97 nm, emission is solely produced by C_2H^*. The CH(A-X) emission is observed right at the energy threshold (96.6 nm) of the $CH^*(A) + CH(X)$ process. The C_2(C-A) emission is observed at 92.3 and 95.5 nm that is produced by the molecular elimination process associated with superexcited state(s). The hydrogen Balmer series are observed at excitation wavelengths much shorter than the expected wavelength thresholds. Continuous emissions, possibly from excited $C_2H_2^+$ ions, are observed at excitation wavelengths shorter than 70 nm. The source of the continuous emissions is subject to further study. The fluorescence spectra produced by two-photon excitation are quite different from those of one-photon excitation at equivalent photon energies. The superexcited states are not reached by the two-photon excitations at 193 and 157.5 nm.

Acknowledgement

This paper is based on the work supported by the NSF and the NASA. The synchrotron radiation facility at the University of Wisconsin is also supported by the NSF.

REFERENCES

1. H. Okabe, *Photochemistry of Small Molecules,* (Wiley, New York, 1978).
2. H. Okabe, J. Chem. Phys. **62**, 2782 (1975).
3. M. Suto and L. C. Lee, J. Chem. Phys. **80**, 4824 (1984), and references therein.
4. P. H. Metzger and G. R. Cook, J. Chem. Phys. **41**, 642 (1964).
5. R. Botter, V. H. Dibeler, J. A. Walker, and H. M. Rosenstock, J. Chem. Phys. **44**, 1271 (1966).
6. J. Berkowitz, *Photoabsorption, Photoionization and Photoelectron Spectroscopy,* (Academic, New York, 1979).
7. R. Unwin, I. Khan, N. V. Richardson, A. M. Bradshaw, L. S. Cederbaum, and W. Domcke, Chem. Phys. Lett. **77**, 242 (1981).
8. J. Kreile, A. Schweig, and W. Thiel, Chem. Phys. Lett. **79**, 547 (1981).
9. A. C. Parr, D. L. Ederer, J. B. West, D. M. P. Holland, and J. L. Dehmer, J. Chem. Phys. **76**, 4349 (1982).
10. D. M. P. Holland, J. B. West, A. C. Parr, D. L. Ederer, R. Stockbauer, R. D. Buff, and J. L. Dehmer, J. Chem. Phys. **78**, 124 (1983).
11. T. Hayaishi, S. Iwata, M. Sasanuma, E. Ishiguro, Y. Morioka, Y. Iida, and M. Nakamuara, J. Phys. B: At. Mol. Phys. **15**, 79 (1982).
12. P. W. Langhoff, B. V. McKoy, r. Unwin, and A. M. Bradshaw, Chem. Phys. Lett. **83**, 270 (1981).
13. L. E. Machado, E. P. Leal, G. Csanak, B. V. McKoy, and P. W. Langhoff, J. Elect. Spectrom. Relat. Phenom. **25**, 1 (1982).
14. C. Y. r. Wu and D. L. Judge, J. Chem. Phys. **82**, 4495 (1985).
15. R. W. Schmieder, J. Chem. Phys. **76**, 2900 (1982).
16. M. Suto, X. Wang, and L. C. Lee, J. Chem. Phys. **85**, 4228 (1986).
17. C. Ye, M. Suto, and L. C. Lee, J. Chem. Phys. **89**, 2797 (1988).

18. J. A. R. Samson, *Techniques of Vacuum Ultraviolet Spectroscopy*, (Wiley, New York, 1967).

19. J. B. Nee, X. wang, M. Suto, and L. C. Lee, Chem. Phys. **113**, 265 (1987).

20. L. C. Lee, J. Phys. B: At. Mol. Phys. **10**, 3033 (1977).

21. L. C. Lee, R. W. Carlson, and D. L. Judge, J. Phys. B: At. Mol. Phys. **9**, 855 (1976).

22. M. W. Chase, Jr., C. A. Davies, J. R. Downey, Jr., D. J. Frurip, R. A. McDonald, and A. N. Syvarud, J. Phys. Chem. Reference Data, **14**, Suppl 1 (1985).

23. K. P. Huber and G. Herzberg, *Constants of Diatomic Molecules*, (Van Nostrand Reinhold, New York, 1979).

24. C. E. Moore, *Atomic Energy Levels*, Vol 1, NSRDS-NBS 35, (GPO Washington D.C. 1971).

25. K. H. Becker, D. Haaks, and M. Schürgers, Z. Naturforsch A **26**, 1770 (1971).

26. Y. Saito, T. Hikida, T. Ichimura, and Y. Mori, J. Chem. Phys. **80**, 31 (1984).

27. R. K. Sander, J. J. Tiee, C. R. Quick, r. J. Romero, and R. Estler, J. Chem. Phys. **89**, 3495 (1988).

28. H. M. Rosenstock, K. Draxl, B. W. Steiner, and J. T. Herron, J. Phys. Chem. Ref. Data, **6**, Suppl. No. 1 (1977).

29. C. Baker and D. w. Turner, Proc. Roy. Soc. **A 308**, 19 (1968).

30. C. K. Ingold and G. W. King, J. Chem. Soc. p. 2702 (1953).

31. W. E. Kammer, Chem. Phys. Lett. **6**, 529 (1970).

32. D. Demoulin, Chem. Phys. **11**, 329 (1975).

33. R. W. Wetmore and H. F. Schaefer, J. Chem. Phys. **69**, 1648 (1978).

34. A. M. Wodtke and Y. T. Lee, J. Phys. Chem. **89**, 4744 (1985).

35. J. R. McDonald, A. P. Baronavski, and V. M. Donnelly, Chem. Phys. **33**, 161 (1978).

36. H. Okabe, R. J. Cody, and J. E. Allen, Jr., Chem. Phys. **92**, 67 (1985).

Table I. Calculated threshold energies and wavelengths for photodissociative excitation processes of C_2H_2. The wavelengths that start to produce emissions from the excited photofragments are also listed.

Processes	Energy (eV)	Wavelength (nm)	
		Calculated	Observed
1. $C_2^*(d) + H_2$	8.81	140.7	
2. $C_2H^* + H$			136.5[a]
3. $C_2^*(C) + H_2$	10.58	117.2	95.5
4. $C_2^*(D) + H_2$	11.69	106.1	92.3
5. $CH^*(A) + CH$	12.84	96.6	95.5
6. $CH^*(B) + CH$	13.20	93.9	92.3
7. $C_2^*(d) + 2H$	13.34	92.9	92.3
8. $CH^*(C) + CH$	13.91	89.1	83.4
9. $C_2^*(C) + 2H$	15.11	82.0	
10. $C_2^*(D) + 2H$	16.22	76.4	
11. $CH^*(A) + C+H$	16.35	75.8	
12. $C_2H + H^*(n=3)$	16.95	73.1	58.7
13. $C_2H + H^*(n=4)$	17.61	70.4	
14. $C_2H + H^*(n=5)$	17.91	69.2	
15. $C_2+H + H^*(n=3)$	22.94	54.1	
16. $C_2H_2^+(\tilde{X}) + e$	11.398	108.77	
17. $C_2H_2^{+*}(\tilde{A}) + e$	16.36	75.8	70 (?)
18. $C_2H_2^{+*}(\tilde{B}) + e$	18.38[b]	67.5	
19. $C_2H_2^{+*}(\tilde{C}) + e$	23.5	52.8	

a. The experimental value given by Suto and Lee (Ref. 3)

b. The Rydberg limit is 18.7 eV as indicated in Fig. 1 (Refs. 12 and 13).

Table II. Electrically-excited photofragments observed at various excitation wavelengths.

Wavelengths (nm)	Excited species
124	C_2H^*
99.1	C_2H^*
95.5	CH(A), C_2(C), C_2H^*
92.3	CH(A, B), C_2(C, d, D), C_2H^*
83.4	CH(A, B, C), C_2 (C, d, D)
76.5	"
68.5	"
66.2	"
63.7	"
58.7	CH(A), C_2(d), H Balmer
55.1	CH(A), C_2(d), H Balmer $C_2H_2^{+*}$(?)
52.7	"
45.7	"
193 (2-photon)	CH(A, B)
157 (2-photon)	CH(A), C_2(d)

Figure Captions

Fig. 1. (a) Absorption and fluorescence cross sections of C_2H_2 in the 50-106 nm region measured with a spectral resolution of 0.2 nm. The cross section is in units of Mb (10^{-18} cm^2). The wavelength positions of Rydberg states calculated by Langhoff *et al.* (Refs. 12 and 13) are indicated. (b) Fluorescence quantum yield.

Fig. 2. Total fluorescence intensities as a function of C_2H_2 pressure observed at the excitation wavelengths indicated.

Fig. 3. Fluorescence spectra from excitation of C_2H_2 at (a) 124 nm and (b) 99.1 nm with spectral resolutions of 1 and 1.5 nm, respectively. $[C_2H_2]$ = 20 mTorr.

Fig. 4. Fluorescence spectra from excitation of C_2H_2 at (a) 95.5 nm and (b) 92.3 nm with spectral resolutions of 1.5 and 1.25 nm, respectively. The C_2H_2 pressures were (a) 20 mTorr and (b) 12 mTorr. The wavelength positions of the CH(A, B-X), C_2(C-A) and C_2(d-a) are indicated.

Fig. 5. Fluorescence spectra from excitation of C_2H_2 at (a) 83.4 nm, (b) 76.5 nm and (c) 68.5 nm. The spectral resolution was 1.25 nm, and the C_2H_2 pressure was 12 mTorr for every spectrum.

Fig. 6. Fluorescence spectrum at 76.5 nm. The spectral resolution was 0.25 nm and the C_2H_2 pressure was 20 mTorr. The wavelength positions of the C_2(C-A), C_2(d-a) and CH(A-X) emission bands are indicated.

Fig. 7. Fluorescence spectra at (a) 58.7 nm, (b) 55.1 nm, and (c) 52.7 nm. The spectral resolutions and the C_2H_2 pressures were 1.5 nm and 12 mTorr for (a), and 1.0 nm and 20 mTorr for (b) and (c). The wavelength positions of the hydrogen Balmer series were indicated.

Fig. 8. Fluorescence spectrum at 45.7 nm. The spectral resolution was 1.5 nm and the C_2H_2 pressure was 20 mTorr.

Fig. 9. Fluorescence spectra from the two-photon excitation of C_2H_2 at (a) 193 nm (ArF laser) and (b) 157.5 nm (F_2 laser). The spectral resolution was 3.3 nm, and the fluorescence was detected by an optical multichannel analyzer.

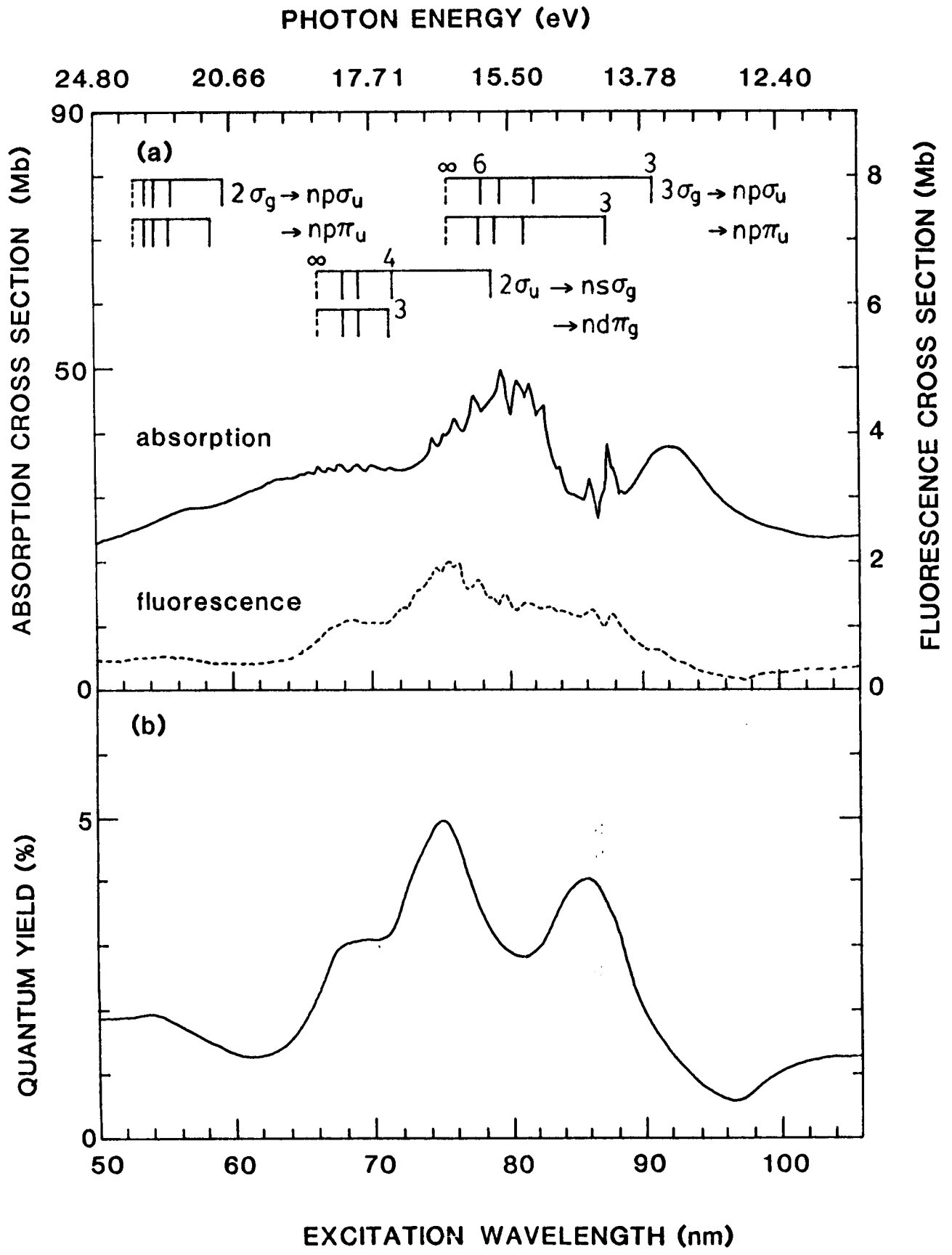
PHOTON ENERGY (eV)
24.80
20.66
17.71
15.50
13.78
12.40
(a)
2σg → npσu
→ npπu
∞ 6 3
3
3σg → npσu
→ npπu
∞ 4
3
2σu → nsσg
→ ndπg
absorption
fluorescence
ABSORPTION CROSS SECTION (Mb)
FLUORESCENCE CROSS SECTION (Mb)
90
50
0
8
6
4
2
0
(b)
QUANTUM YIELD (%)
5
0
50
60
70
80
90
100
EXCITATION WAVELENGTH (nm)

Fig. 1

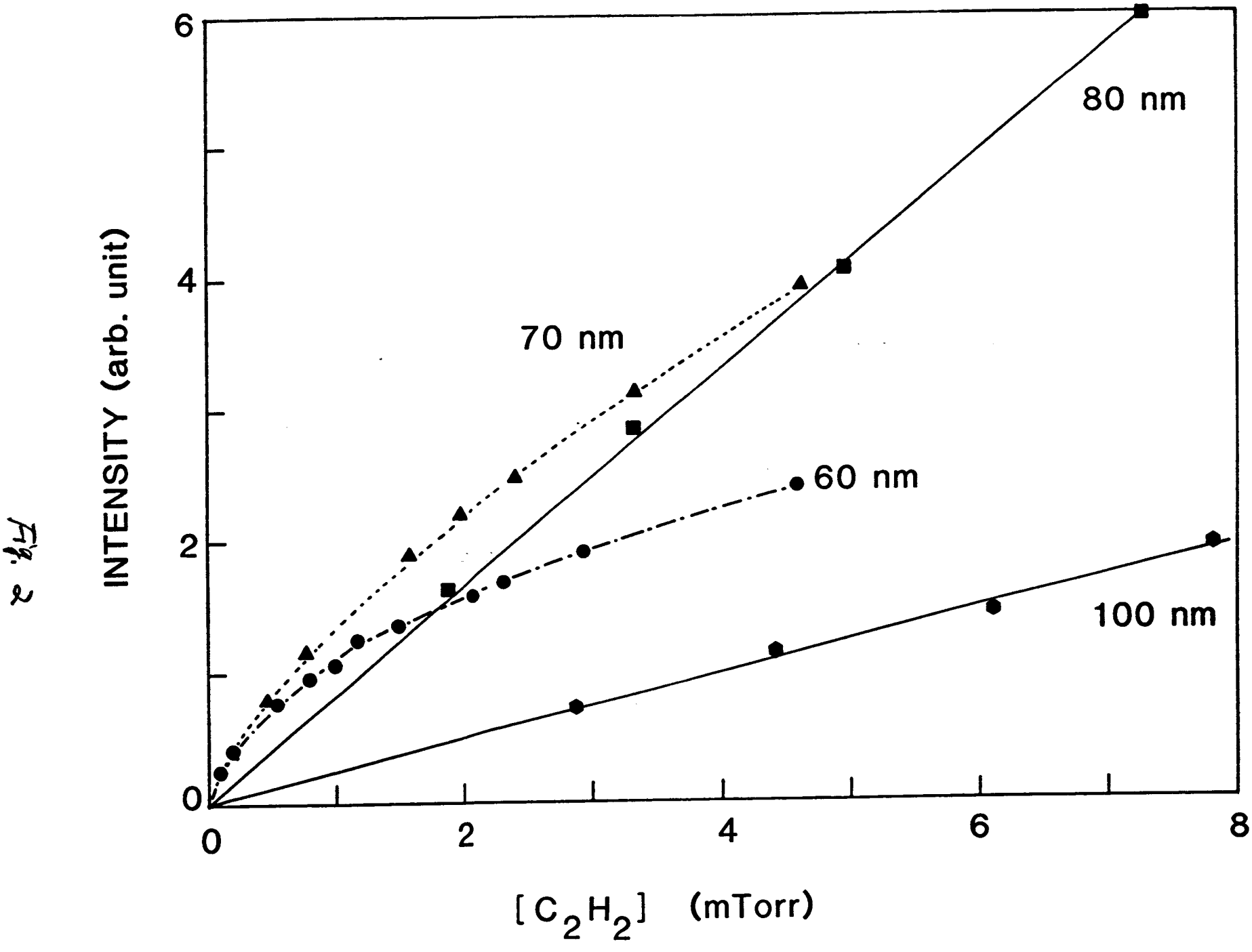
INTENSITY (arb. unit)
6
4
2
0
0
2
4
6
8
80 nm
70 nm
60 nm
100 nm
[C2H2] (mTorr)

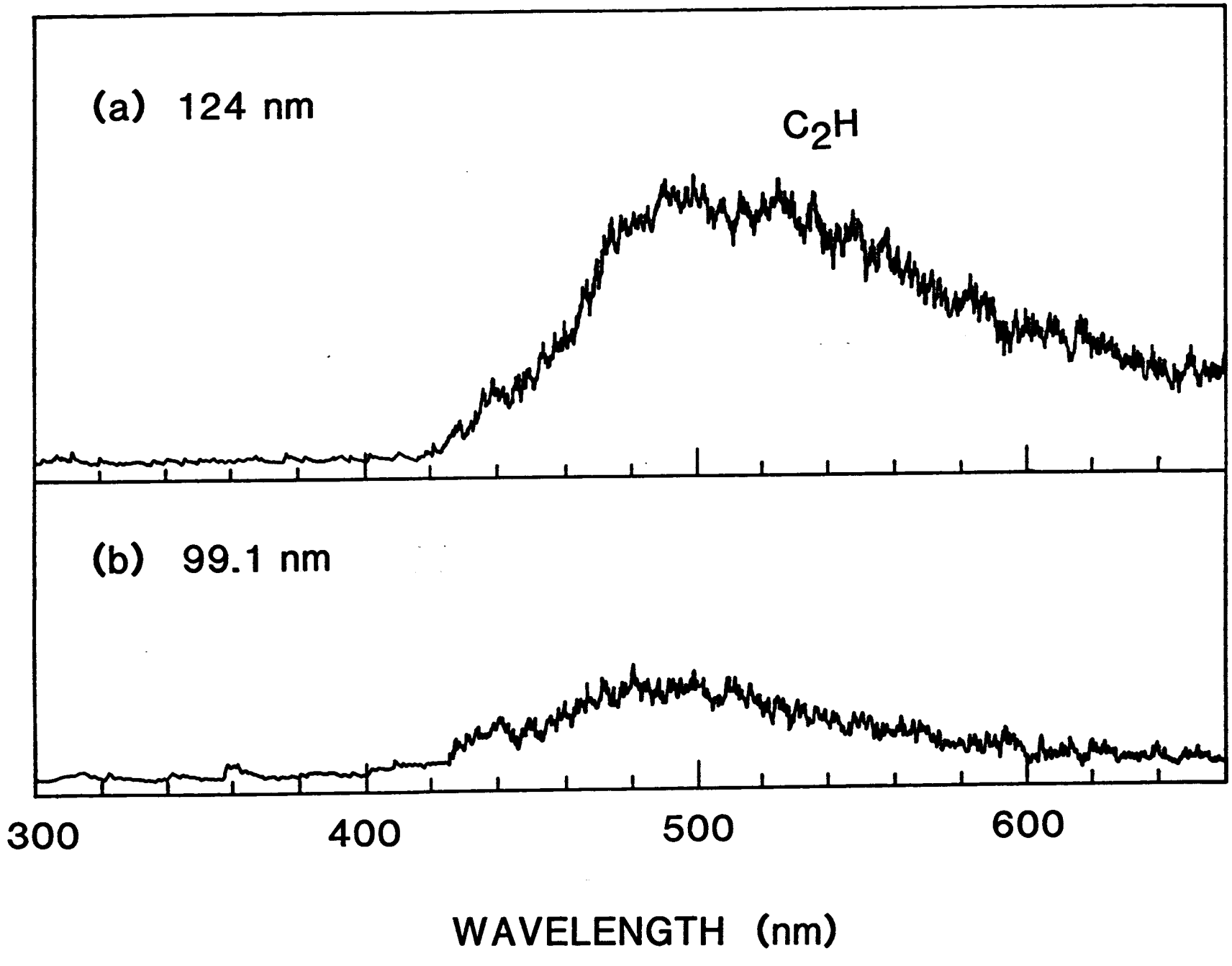

Fig. 3

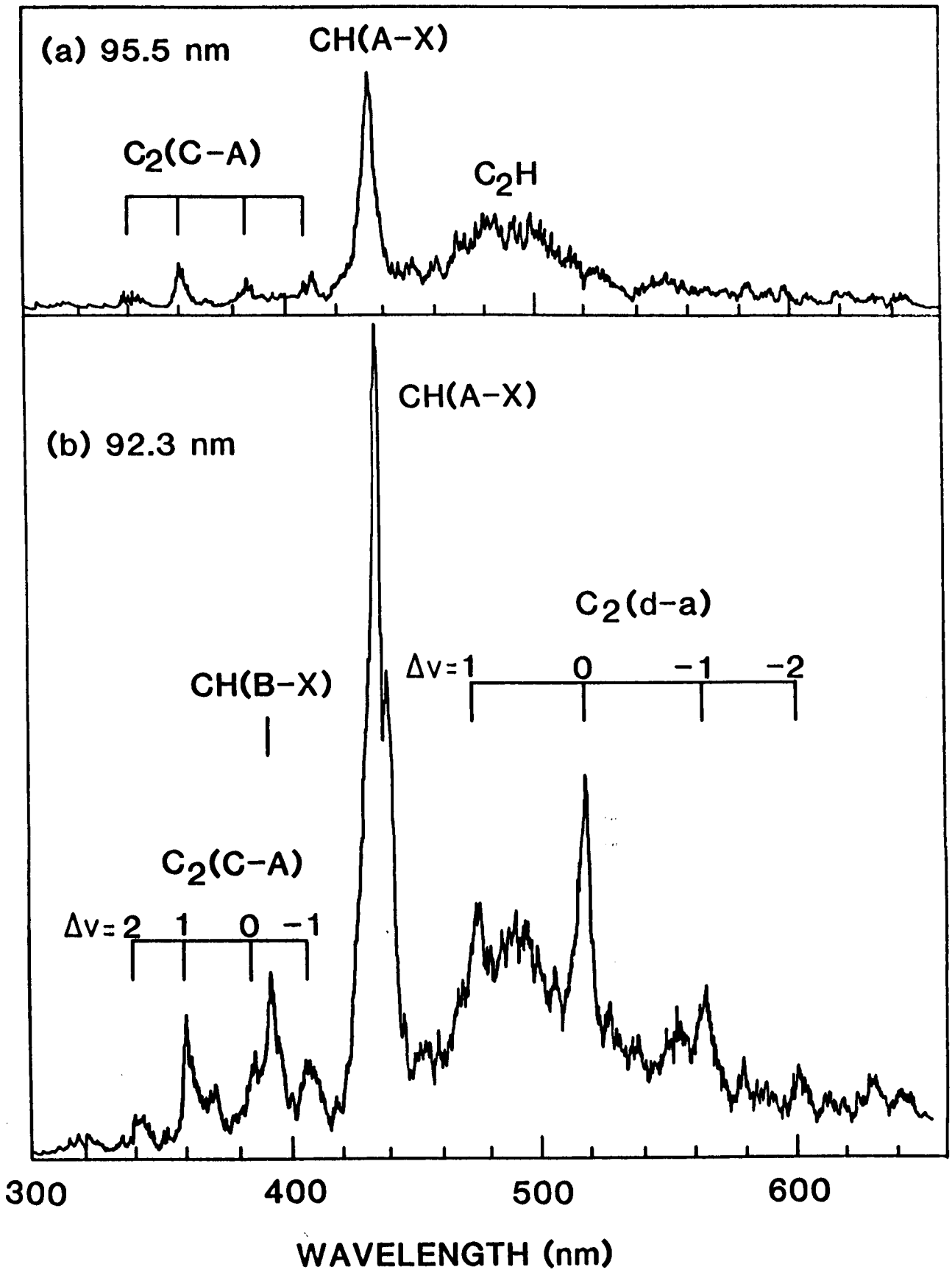
(a) 95.5 nm
CH(A-X)
C2(C-A)
C2H
(b) 92.3 nm
CH(A-X)
C2(d-a)
Δv=1 0 -1 -2
CH(B-X)
C2(C-A)
Δv=2 1 0 -1
300
400
500
600
WAVELENGTH (nm)

Fig. 4

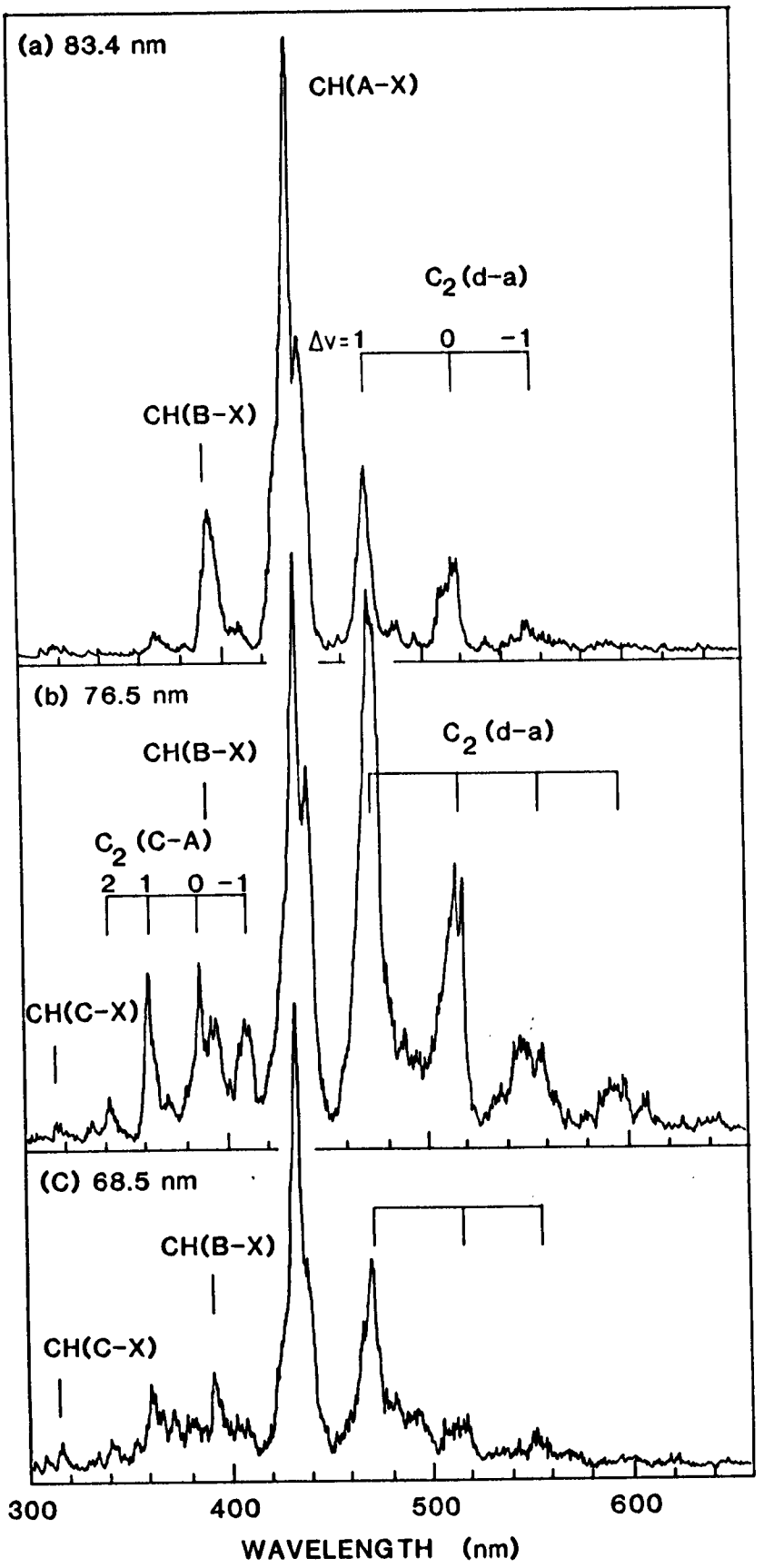
(a) 83.4 nm
CH(A-X)
C2 (d-a)
Δv=1 0 -1
CH(B-X)
(b) 76.5 nm
CH(B-X)
C2 (d-a)
C2 (C-A)
2 1 0 -1
CH(C-X)
(C) 68.5 nm
CH(B-X)
CH(C-X)
300
400
500
600
WAVELENGTH (nm)

Fig. 5

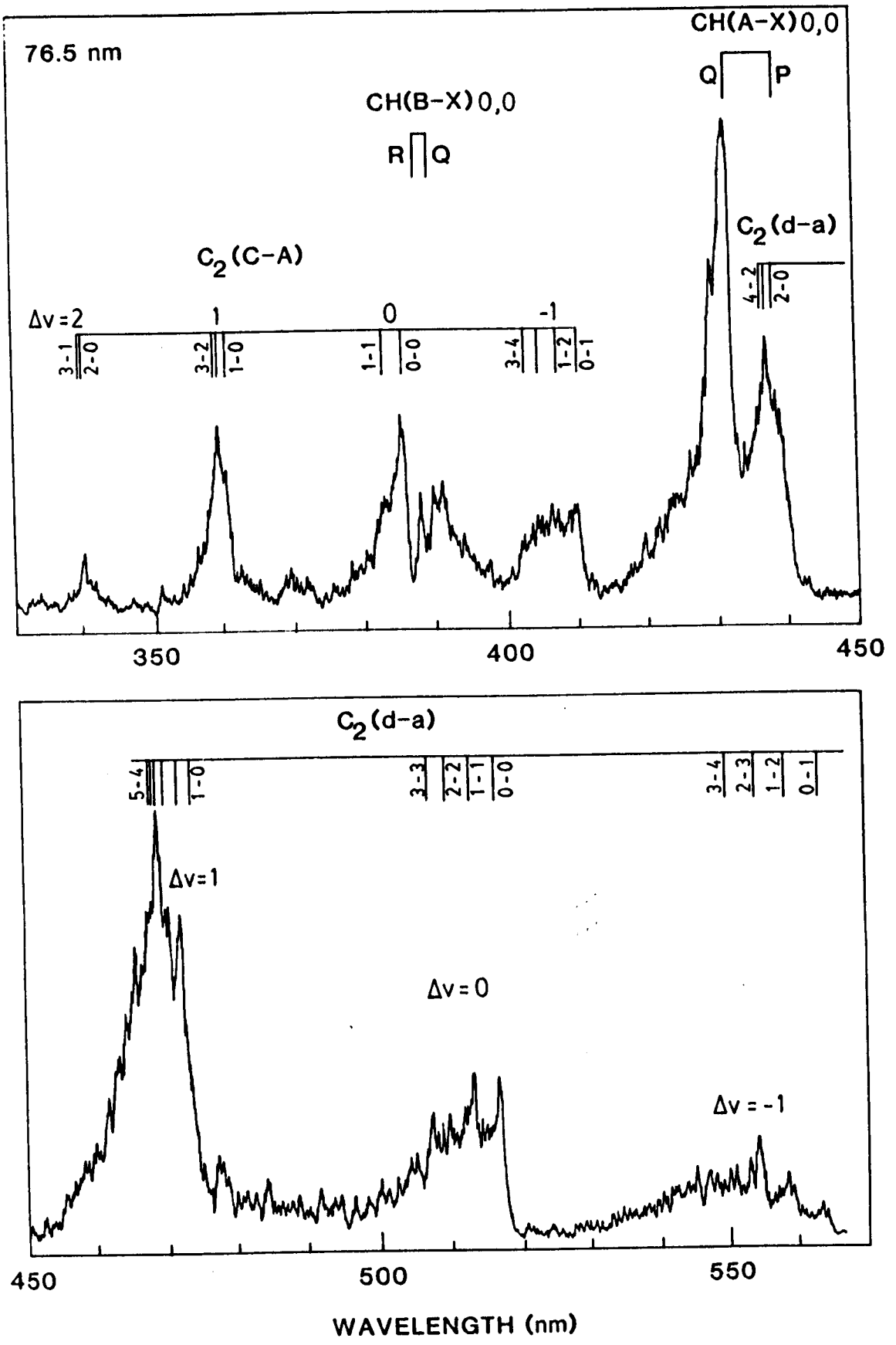
76.5 nm
CH(A-X)0,0
Q
P
CH(B-X)0,0
R
Q
C2(d-a)
C2(C-A)
Δv=2
1
0
-1
3-1
2-0
3-2
1-0
1-1
0-0
3-4
1-2
0-1
4-2
2-0
350
400
450
C2(d-a)
5-4
1-0
3-3
2-2
1-1
0-0
3-4
2-3
1-2
0-1
Δv=1
Δv=0
Δv=-1
450
500
550
WAVELENGTH (nm)

Fig. 6

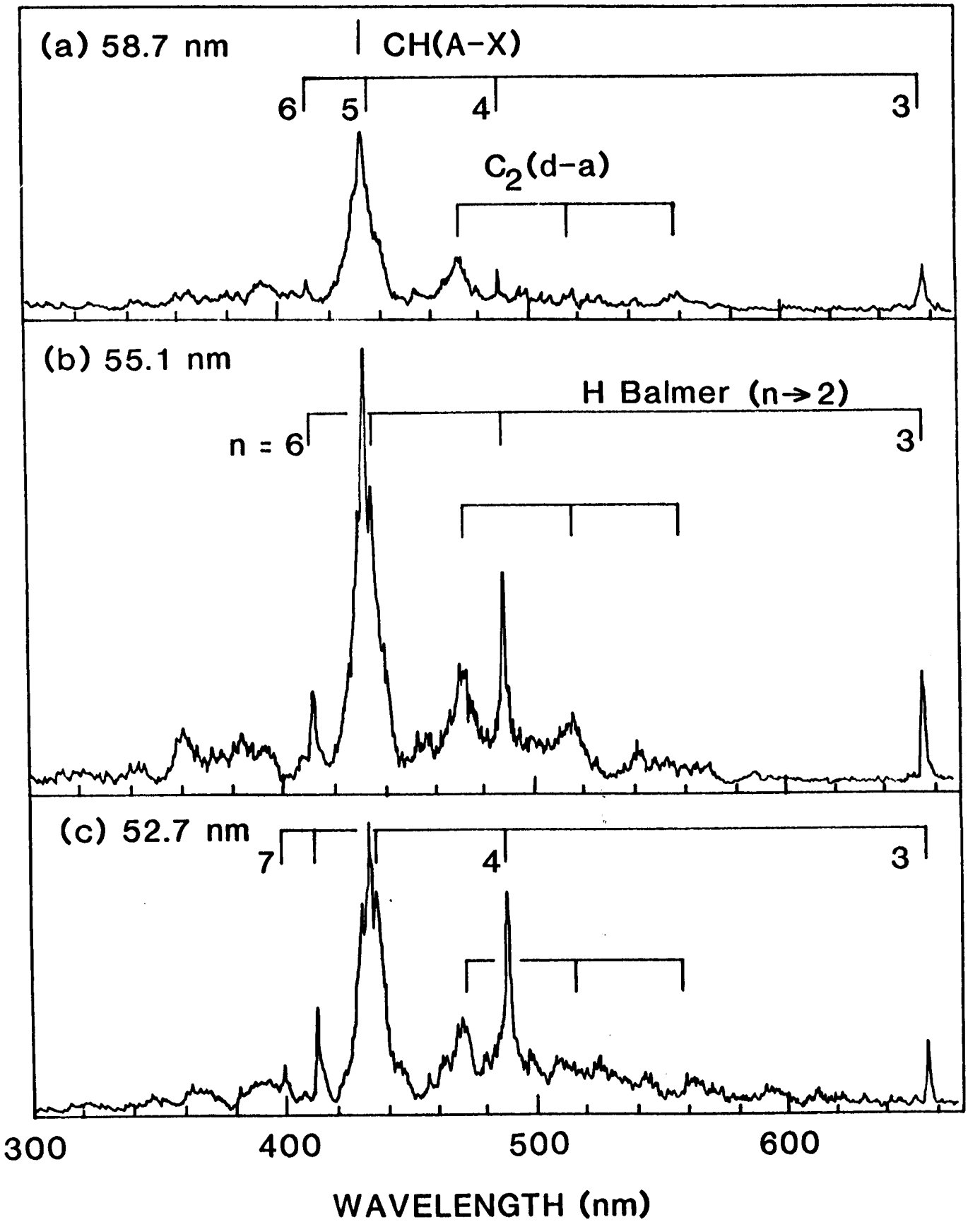
(a) 58.7 nm
CH(A-X)
6
5
4
3
C_2(d-a)
(b) 55.1 nm
H Balmer (n→2)
n = 6
3
(c) 52.7 nm
7
4
3
300
400
500
600
WAVELENGTH (nm)

Fig. 7

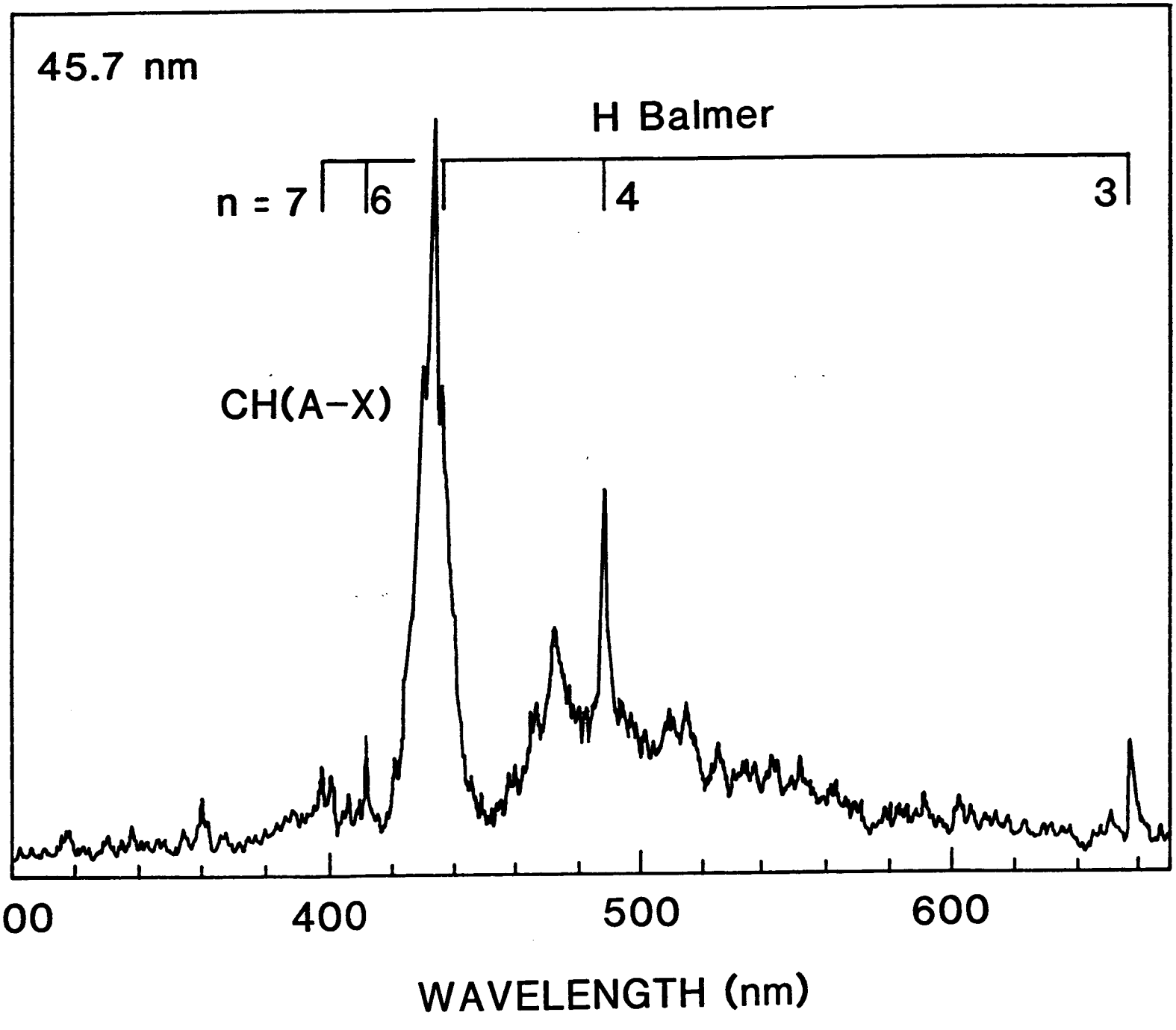
45.7 nm
H Balmer
n = 7
6
4
3
CH(A-X)
300
400
500
600
WAVELENGTH (nm)

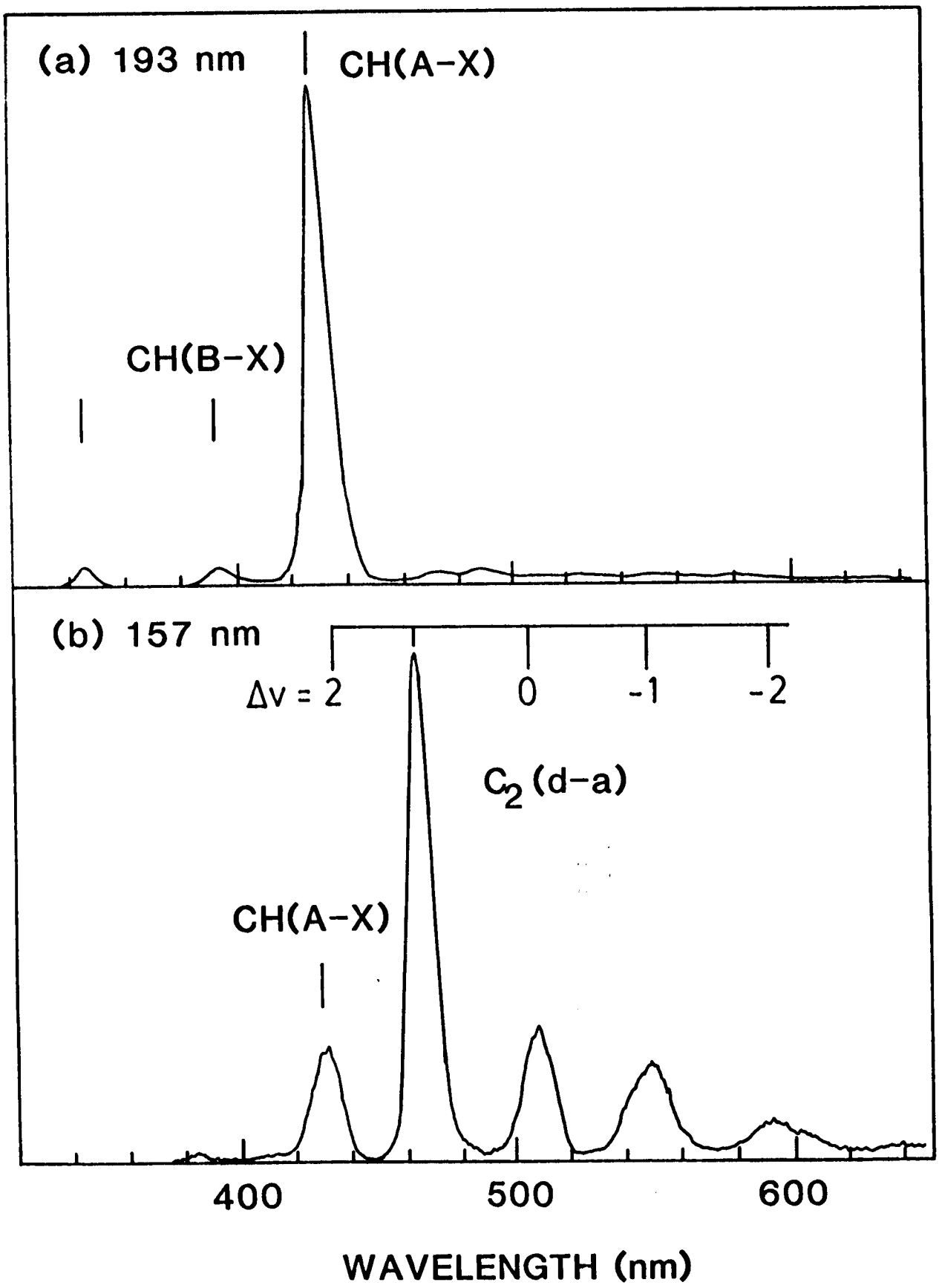
(a) 193 nm
CH(A-X)
CH(B-X)
(b) 157 nm
Δv = 2
0
-1
-2
C2 (d-a)
CH(A-X)
400
500
600
WAVELENGTH (nm)

Fig. 9